Clouds

Stephan de Roode

September 7, 2004

Part I - Theoretical background and governing equations

Preface

Water is a very important component of the Earth's atmosphere as its phase changes can produce liquid water and ice clouds. To account for latent heat effects in clouds variables that are conserved for adiabatic processes that involve phase changes are often used in meteorology. In Part I we will summarize a few frequently used conserved variables for heat. In addition, water in its three phases (vapor, liquid and ice) affects the density of air. As much of the thermodynamics applied to the atmosphere involves the first and second laws of thermodynamics, the ideal gas law, or Dalton's law of partial pressures, a short summary of basic thermodynamics will be presented.

A few simple exercises are included. Basically, most of them are intended to give the student some feeling for the physical meaning of mathematically derived equations, or to obtain some appreciation for 'typical' numbers in this field of research.

Part I presents the basic thermodynamics necessary for further study of cloud systems. It merely gives a summary and can therefore not be considered as a substitute for a text book. A book that is entirely dedicated to atmospheric thermodynamics is the one by Bohren and Albrecht (1998). According to these authors, 'the prevailing view of textbooks is that they should be as boring as possible ... They seem to be written with the aim of making science as uninteresting as possible so that their authors can then wring their hands over the lack of interest shown by young people in science.' As this text sample from their preview readily suggests, the book is written in a rather provocative way, and gives, besides equations, a bunch of interesting anecdotal facts. The former author is also the writer of 'Clouds in a glass of beer', which title may sound as a recommendation to students, and is frequently quoted in Karel Knip's 'Alledaagse Wetenschap' contribution to the dutch newspaper NRC Handelsblad. Another book that gives a thorough overview of the topic is provided by Iribarne and Godson (1981). Some of the material discussed in these short notes can also be found in several popular meteorology text books, like Holton (1992) and Gill (1982). Some parts were inspired by the thermodynamics course presented by Bjorn Stevens at UCLA.

Chapter 1

Basic thermodynamics: A summary

The ideal gas law and the first and second law of thermodynamics will be discussed briefly. The Clausius-Clapeyron equation is derived to obtain the dependency of the water vapor saturation pressure on the temperature.

1.1 Equation of state: The ideal gas law

The equation of state for an ideal gas law relates its pressure p, volume V and temperature T by

$$pV = NkT = \nu R^* T, \tag{1.1}$$

where N is the number of identical molecules, ν is the number of moles of gas, $k = 1.3806{\times}10^{-23}$ J K $^{-1}$ is Boltzmann's constant, $R^* \equiv N_a k = 8.341$ J mol^{-1} K^{-1} is the universal gas constant, with $N_a = 6.022 \times 10^{23}$ mol $^{-1}$ Avogadro's number. The Earth's atmosphere is a mixture of gases, mostly nitrogen, oxygen and argon, trace gases like carbon dioxide, ozone and methane, and variable amounts of water in its three physical phases. The concentrations of the mixture of gases that we define as dry air (see Table 1.1) are very closely constant up to a height of about 100 km. The dry atmosphere can be taken to a very good approximation as an ideal gas.

In general, it is useful to formulate the thermodynamic relations in terms of *intensive* variables. An intensive variable is one whose value does not depend on the amount of matter in the system, like the temperature of pressure. In contrast, an *extensive* variable, depends on the size of the system. For instance, the internal energy of a gas is an extensive variable since if we double its size, all else being kept

Gas	Molecular weight M_i [g mol^{-1}]	Molar fraction	Mass fraction m_i/m_{tot}	Specific gas constant R_i [J kg^{-1} K^{-1}]	$(m_i/m_{tot})R_i$ [J kg^{-1} K^{-1}]
NO_2	28.013	0.7809	0.7552	296.80	224.15
O_2	31.999	0.2095	0.2315	259.83	60.15
Ar	39.948	0.0093	0.0128	208.13	2.66
CO_2	44.010	0.0003	0.0005	188.92	0.09
total		1.0000	1.0000		287.05

Table 1.1: Main components of dry atmospheric air (source *Smithsonian Meteorological Tables*).

equal, its internal energy will double. Given a system whose volume V contains an amount of mass M,

$$v = \frac{V}{M} \tag{1.2}$$

denotes the *specific volume* of the system. In principle, every extensive variable can be converted to its corresponding intensive form by normalizing it by the amount of matter it describes. In the remainder of this text we will use lower case letters to denote specific intensive quantities, as opposed to their non-intensive counterpart for which we will use capital letters, e.g. the specific volume v and the volume V.

We would like to write the gas law in terms of kilograms rather than moles. To this end, we need use the molecular weight of a species i, M_i (g/mol), and gives the mass of 1 mole of identical molecules in grams. If the total mass of the gas is m_i, we can express the gas law as,

$$pV = \frac{m_i}{M_i} R^* T. \tag{1.3}$$

The molecular weight can be substituted out by using the *specific gas constant* R_i for a species i, which is defined as

$$R_i \equiv R^*/M_i. \tag{1.4}$$

For a mixture of gases the partial pressure p_i of the i^{th} gas is defined as the pressure p_i that it would have if the same mass (m_i) existed alone at the same temperature T and occupying the same volume V. By (1.3) and (1.4) the partial pressure for an ideal gas can thus be expressed as

$$p_i = \frac{T}{V} m_i R_i. \tag{1.5}$$

According to Dalton's law of partial pressures, the total pressure p of a mixture of (ideal) gases is the sum of the pressures $\sum p_i$ of each species i as if it alone

occupied a volume V,

$$p = \frac{T}{V} \sum_i m_i R_i = \rho R_m T, \tag{1.6}$$

in which $m_{tot} = \sum_i m_i$ the total mass, $R_m = 1/m_{tot} \sum_i m_i R_i$ the specific gas constant for the mixture, and $\rho = m_{tot}/V$ is the density. Eq. (1.6) is the form of the gas law generally used in meteorology. Table 1.1 shows the value of the gas constant for dry air, $R_d = 287.05$ J kg^{-1} K^{-1}. The specific gas constant for water vapor $R_v = 461.5$ J kg^{-1} K^{-1}.

1.2 The first law of thermodynamics

The first law of thermodynamics is equivalent to conservation of energy. It states that the internal energy of a closed system (U) can change only if heat (Q) is added or if work (W) is done on the system by its surroundings,

$$dU = dQ + dW. \tag{1.7}$$

The rate of work is given by

$$dW = -pdV, \tag{1.8}$$

such that (1.7) can be expressed as

$$dU = dQ - pdV. \tag{1.9}$$

Usually the ideal gas law is utilized to recast (1.9) in terms of measurable physical parameters.

1.2.1 Rules for differentiating

If the equation of state is governed by three variables (p, v, T) then we can write

$$p = f_1(v, T) \quad , \quad v = f_2(p, T) \quad \text{or} \quad T = f_3(p, v). \tag{1.10}$$

In other words, there are only two independent state variables,

$$dp = \frac{\partial f_1}{\partial v} dv + \frac{\partial f_1}{\partial T} dT \ , \ dv = \frac{\partial f_2}{\partial p} dp + \frac{\partial f_1}{\partial T} dT \ , \ dT = \frac{\partial f_3}{\partial p} dp + \frac{\partial f_1}{\partial v} dv. \tag{1.11}$$

If we differentiate state variables other than p, v, or T, for instance, the specific internal energy u, we must specify which set of thermodynamics parameters we use. Otherwise $(\partial u/\partial p)$ is ambiguous and depends on the choice of thermodynamic coordinates, for example whether u is defined as a function of p and v or as a

function of p and T. To express the rate of change of u as a result of an isobaric process, i.e. a change in the pressure p, we write

$$\frac{\partial u(p,T)}{\partial p} \equiv \left(\frac{\partial u}{\partial p}\right)_T \tag{1.12}$$

meaning that p and T are chosen as thermodynamical coordinates and that the the temperature is held constant for this process.

1.2.2 Enthalpy and specific heat

A measure of the quantity of heat needed to raise the temperature of one gram of a substance by 1 °C is called the heat capacity C, and is defined as:

$$C = dQ/dT. \tag{1.13}$$

But this definition is incomplete. There are many ways to add heat to a system. One could add heat to a system at constant volume or at constant pressure. Or one could add heat to a system even at constant temperature. One could add heat as both the volume and pressure change. The specific heat capacity at constant pressure, c_p and the specific heat capacity at constant volume, c_v are different.

If one choses the specific volume v and the temperature T as thermodynamic coordinates, then the specific internal energy u can be expressed as,

$$du = \left(\frac{\partial u}{\partial v}\right)_T dv + \left(\frac{\partial u}{\partial T}\right)_v dT = \left(\frac{\partial u}{\partial v}\right)_T dv. \tag{1.14}$$

where the last equality follows from the fact that the internal energy of an ideal gas does not depend on its volume (see exercise 2),

$$\left(\frac{\partial u}{\partial v}\right)_T = 0. \tag{1.15}$$

It must be stressed that (1.15) implicitly assumes that the intermolecular forces are negligibly small, and therefore is applicable only to an ideal gas.

The density in the gas law (1.6) can be replaced by the specific volume with aid of (1.2), such that $pv = RT$. Substituting this form into (1.9) and using (1.14) gives

$$dq = \left(\frac{\partial u}{\partial T}\right)_v dT + pdv, \tag{1.16}$$

where dq indicates the differential amount of heat added. For an *isometric* process $dv = 0$, and if we define $dq = c_v dT|_v$, then the isometric specific heat c_v follows from (1.16),

$$c_v \equiv \left(\frac{\partial u}{\partial T}\right)_v. \tag{1.17}$$

Another state variable that is often used in atmospheric thermodynamics is the *enthalpy* h

$$h = u + pv. \tag{1.18}$$

Given this definition, the first law can be expressed as

$$dq = du + pdv = dh - d(pv) + pdv = dh - vdp. \tag{1.19}$$

For an isobaric process $dp = 0$, and consequently $dq = dh$. The isobaric specific heat c_p is defined as

$$c_p \equiv \left(\frac{\partial h}{\partial T}\right)_p, \tag{1.20}$$

For a constant pressure process a specific volume change dv and a change in the temperature dT are related as

$$pdv = RdT|_p. \tag{1.21}$$

Eqs. (1.17) and (1.21) can be substituted into (1.16) to give

$$dq = (c_v + R)dT|_p = dh, \tag{1.22}$$

where the last equality follows from (1.19). By the definition for c_p according to (1.20) it follows that

$$c_p = c_v + R. \tag{1.23}$$

The enthalpy gives a measure of total potential energy of the atmosphere. As an explanation, let us consider the total internal energy (per unit cross-sectional area) of the entire atmosphere,

$$U = \int_0^\infty \rho c_v T dz. \tag{1.24}$$

Likewise, the total gravitational energy reads

$$P = \int_0^\infty \rho g z dz. \tag{1.25}$$

If we assume that the atmosphere is in a hydrostatic equilibrium, $dp/dz = -\rho g$, we can rewrite (1.25) as

$$P = -\int_0^\infty z\frac{dp}{dz}dz. \tag{1.26}$$

Integration by parts yields

$$P = \int_0^\infty p dz. \tag{1.27}$$

Substitution of the ideal gas law gives

$$P = \int_0^\infty \rho R T dz, \tag{1.28}$$

such that the sum of the internal energy and the potential energy becomes

$$U + P = \int_0^\infty \rho(c_v + R)T dz = \int_0^\infty \rho h dz = H_{tot}. \tag{1.29}$$

The total enthalpy of the an atmospheric column is therefore given by the sum of its total internal energy and gravitational potential energy. This can be interpreted as follows. If the atmosphere is heated, its enthalpy increases for two reasons: Its internal energy increases, and its potential energy increases because the center of mass rises. Many processes in the atmosphere are nearly isobaric, which is why the enthalpy is more relevant to our applications than the internal energy.

Exercise 1. Lorenz (1955) defined the available potential energy of the atmosphere as the difference between the actual enthalpy and the minimum total enthalpy that could be achieved by rearranging the mass under reversible adiabatic processes. This definition can be understood by considering the conservation equation for the total energy of the atmosphere (including internal, potential, and kinetic energies). According to this equation, the sum of the kinetic energy per unit mass and the enthalpy of unit mass changes in time due to redistribution of mass within the atmosphere, and also due to to energy sources and sinks such as radiation, latent heating, and surface exchanges. In the absence of energy sources and sinks, the tendency of the total kinetic energy (K) and the total enthalpy (H) is given by,

$$\frac{\partial}{\partial t}(K + H) = 0. \tag{1.30}$$

Consider a simple system containing two parcels of equal mass. In the given state, parcels with potential temperature θ_1 and θ_2 reside at pressures p_1 and p_2, respectively. We assume that $\theta_1 < \theta_2$ and $p_1 < p_2$.

a) Use the definition for the potential temperature to compute the enthalpy $c_p T$ of the two parcels.

The lower parcel 1 moves upwards and becomes adiabatically ($dq = 0$) interchanged with parcel number 2, so that parcel number 2 goes to pressure p_1 and vice versa.

b) Compute the enthalpy of the two parcels after the swapping process. What is the difference with their initial total enthalpy? Can you explain if this process can occur spontaneously, regarding the fact that kinetic energy is needed to interchange the parcels?

Background: This exercise has been taken from a paper by Wang and Randall (1996). These authors utilize the 'parcel swapping' approach to minimize the enthalpy of a given atmospheric column to compute the total potential energy available for cumulus convection.

1.3 The second law of thermodynamics: Entropy

A *reversible* process is defined as

$$\oint \frac{\delta Q}{T} = 0. \tag{1.31}$$

This integral is independent of the path. The entropy S is defined as $dS = dQ/T$, or alternatively, the specific entropy s, $ds = dq/T$. Unlike heat and work, the entropy is a state variable, thus we can speak of the entropy in state A or B. The second law of thermodynamics states that

$$Tds = du + pdv \geq 0. \tag{1.32}$$

Note that by the temperature in the denominator of (1.31) heat and entropy are not linearly related.

What is the relevance of entropy to meteorologists? To answer this question, we define the potential temperature in terms of a measure of the entropy

$$ds = c_p d \ln \theta. \tag{1.33}$$

Next, we use the definition of the internal energy (1.17) and the gas law to give

$$Tds = c_p dT - \frac{R_d T}{p} dp \qquad \Longleftrightarrow \qquad ds = c_p (d \ln T - d \ln p^{\frac{R_d}{c_p}}). \tag{1.34}$$

Integration yields

$$s - s_0 = c_p (\ln \theta - \ln \theta_0) = c_p \ln \left[\frac{T}{T_0} \left(\frac{p_0}{p} \right)^{\frac{R_d}{c_p}} \right]. \tag{1.35}$$

For an isentropic process ($ds = 0$) we immediately see that this is also a constant-potential temperature process. Furthermore, if we set $T_0 = \theta_0$,

$$\theta = T \left(\frac{p_0}{p} \right)^{\frac{R_d}{c_p}}. \tag{1.36}$$

The potential temperature θ can be interpreted as the temperature a parcel would have if it were displaced isentropically to a reference height where the pressure is p_0, which is usually taken $p_0 = 1000$ hPa. In other words, a parcel with temperature T at pressure level p will have a potential temperature θ, which value is equal to the temperature T_0 at the pressure level p_0.

The lapse rate of the potential temperature can be obtained by differentiating (1.36) with respect to height

$$\frac{d\theta}{dz} = \frac{\theta}{T}\left(\frac{dT}{dz} - \frac{R_d T}{pc_p}\frac{dp}{dz}\right) \tag{1.37}$$

Assuming that the atmosphere is in a hydrostatic balance, $dp/dz = -\rho g$, then with aid of the gas law (1.37) can be written as

$$\frac{d\theta}{dz} = \frac{\theta}{T}\left(\frac{dT}{dz} + \frac{g}{c_p}\right). \tag{1.38}$$

Since $g/c_p = \Gamma_d$ is the dry adiabatic lapse rate, we conclude that if the temperature profile follows the dry adiabatic lapse rate, the potential temperature is constant with height.

Figure 1.1 shows observations made in a clear convective boundary layer (CBL). Because of solar radiative heating turbulent eddies are driven from ground surface. The thermals can penetrate into the thermal inversion, which for this case is located at about 380 m, above which they are damped by the stable stratification. Turbulence tends to make the interior of the CBL vertically well-mixed, in the sense that quantities like the potential temperature and the specific humidity become approximately constant with height. For a well-mixed CBL, the temperature follows approximately the dry-adiabatic lapse rate. The potential temperature is vertically well-mixed. Note that in the boundary layer the specific humidity hardly varies with height, whereas the relative humidity tends to increase with height.

Exercise 2. In the derivation of the specific heats we used Eq. (1.15), $(\partial u/\partial v)_T = 0$. Show that this relation applies to an ideal gas. Strategy: write expressions for du and ds as a function of the thermodynamic coordinates p and v, and insert the expression for du into the second law.

1.4 The Clausius-Clapeyron equation

Sometimes it is argued that when air cools clouds form because cold air cannot hold as much water vapor as warm air. Since, for instance, cumulus clouds develop in surface-driven thermals that have gradually cooled during their ascent, it appears that there is a causal relation between cooling and saturation so that this argument

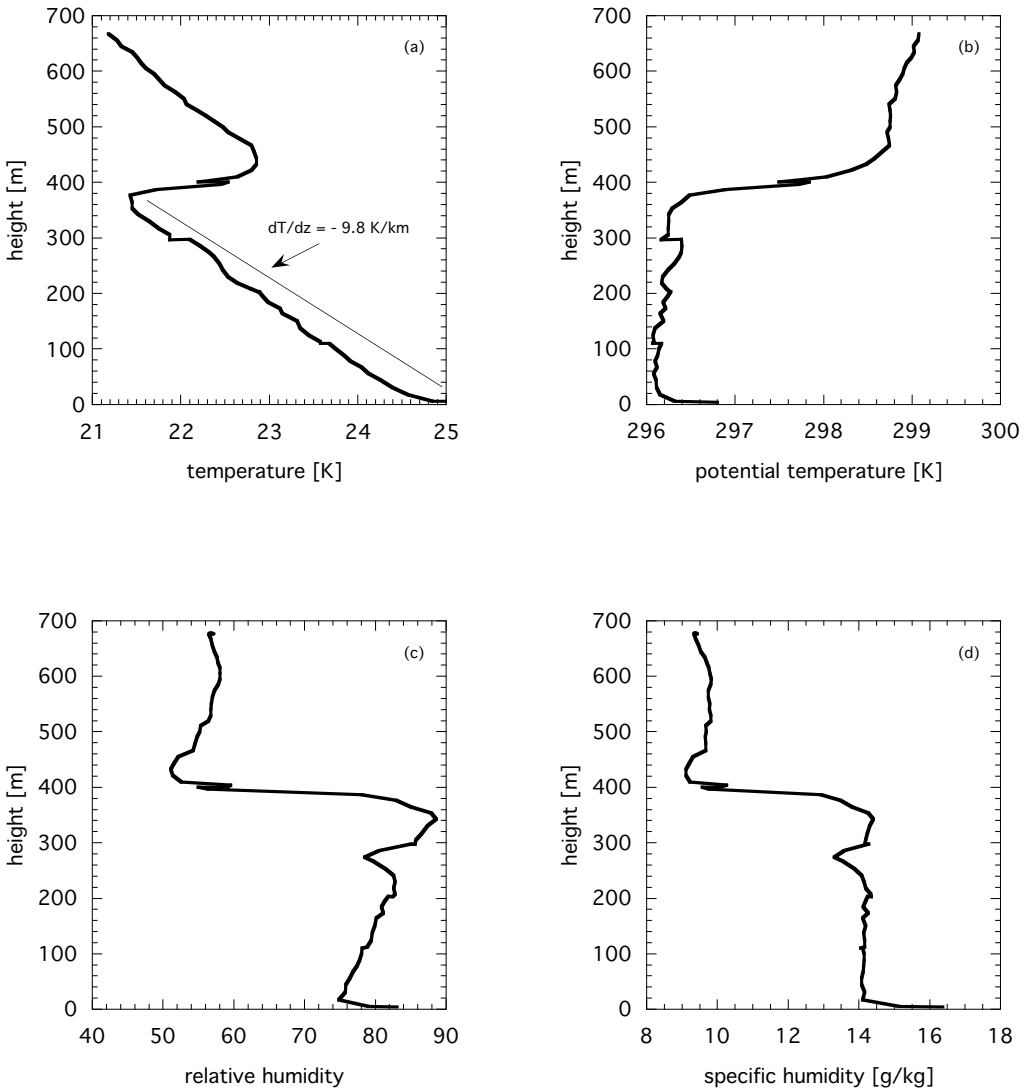

Figure 1.1: Vertical profiles of (a) the temperature T, (b) the potential temperature θ, (c) the relative humidity, and (d) the specific humidity q_v, for a clear convective boundary layer as observed by a tethered balloon at Cabauw, Netherlands, around 10:00 h (local time), 23 August 2001. The thin line indicates the dry-adiabatic temperature lapse rate.

is making sense. However, the underlying notion that air is some kind of imaginary sponge that can absorb an amount of water vapor depending on its temperature is a misconception.

Water molecules are constantly coursing back and forth between phases (another word for the three states: vapor, liquid, and solid). If more molecules are leaving a liquid surface than arriving, there is a net evaporation; if more arrive than leave, a net condensation. It is these relative flows of molecules which determine whether a cloud forms or evaporates. The rate at which vapor molecules arrive at a surface of liquid (cloud drop) or solid (ice crystal) depends upon the *vapor pressure*. The rate at which vapor molecules leave the surface depends upon the characteristics of the surface. What appears to be cloud-free air (virtually) always contains sub microscopic drops, but as evaporation exceeds condensation, the drops do not survive long after an initial chance clumping of molecules. As air is cooled, the evaporation rate decreases more rapidly than does the condensation rate with the result that there comes a temperature (the dew point temperature) where the evaporation is less than the condensation and a droplet can grow into a cloud drop. Evaporation increases with temperature, not because the holding capacity of the air changes, but because the more energetic molecules can evaporate more readily (with, of course, the caveat that evaporation is also influenced by things other than temperature, as described above). (see http://www.ems.psu.edu/ fraser/BadMeteorology.html from which the explanation above is taken, and more nice examples of 'bad' meteorology).

The water vapor pressure is usually denoted by the symbol e, and from the gas law it follows that

$$e = \rho_v R_v T, \tag{1.39}$$

where ρ_v is the density of water vapor. In case the concentration of water vapor is at its saturation value we can define the corresponding saturation vapor pressure by e_s. A familiar quantity to many is the relative humidity RH of air, which is defined as

$$RH = \frac{e}{e_s}. \tag{1.40}$$

Clearly, the relative humidity gives a measure of the ratio of two *(partial) pressures*.

To assess the role of the temperature on e_s, we first need to use the entropy equation, after which we will derive the Clausius-Clapeyron equation. Let us choose v and T as thermodynamic coordinates, such that the specific internal energy can be expressed as

$$du = \left(\frac{\partial u}{\partial T}\right)_v dT + \left(\frac{\partial u}{\partial v}\right)_T dv, \tag{1.41}$$

and likewise for the specific entropy,

$$ds = \left(\frac{\partial s}{\partial T}\right)_v dT + \left(\frac{\partial s}{\partial v}\right)_T dv. \tag{1.42}$$

Substituting (1.41) into the entropy equation (1.32) yields

$$ds = \frac{1}{T}\left(\frac{\partial u}{\partial T}\right)_v dT + \frac{1}{T}\left[\left(\frac{\partial u}{\partial v}\right)_T + p\right] dv. \tag{1.43}$$

From comparison of (1.42) to (1.43) it follows that

$$\left(\frac{\partial s}{\partial T}\right)_v = \frac{1}{T}\left(\frac{\partial u}{\partial T}\right)_v, \tag{1.44}$$

$$\left(\frac{\partial s}{\partial v}\right)_T = \frac{1}{T}\left[\left(\frac{\partial u}{\partial v}\right)_T + p\right]. \tag{1.45}$$

After differentiating (1.44) with respect to v and (1.45) with respect to T and using the chain rule, we obtain

$$\frac{\partial^2 s}{\partial v \partial T} = \frac{1}{T}\frac{\partial^2 u}{\partial v \partial T}, \tag{1.46}$$

$$\frac{\partial^2 s}{\partial T \partial v} = \frac{1}{T}\left[\frac{\partial^2 u}{\partial T \partial v} + \left(\frac{\partial p}{\partial T}\right)_v\right] - \frac{1}{T^2}\left[\left(\frac{\partial u}{\partial v}\right)_T + p\right]. \tag{1.47}$$

Because the cross partial derivatives are equal we get

$$\left(\frac{\partial u}{\partial v}\right)_T = T\left(\frac{\partial p}{\partial T}\right)_v - p. \tag{1.48}$$

This equation will be our starting point to compute the functional dependence of the saturation vapor pressure e_s as a function of temperature. It is essential to note that as we consider liquid water in equilibrium with its vapor we cannot neglect the left-hand-side of (1.48), since this mixture does *not* behave as an ideal gas.

Let us consider a total amount of water $m_v + m_l = m$, with the indices 'v' and 'l' indicating values for water vapor and liquid water, respectively. The total internal energy is then given by the sum of the internal energies of the two components

$$U = m_v u_v + m_l u_l, \tag{1.49}$$

and similarly for the volume

$$V = m_v v_v + m_l v_l. \tag{1.50}$$

We assume that the mixture is kept in an apparatus such as a cylinder fitted with a piston, which as a whole is immersed in a constant-temperature reservoir. If we decrease the volume of the cilinder, the vapor pressure increases until it becomes equal to the saturation vapor pressure e_s. A further decrease in the volume does not lead to a subsequent change in the water vapor pressure. Instead, water vapor is condensed to liquid water. The constant pressure during this process is the saturation vapor pressure.

Suppose we change the volume of the cylinder such that a mass δm evaporates, then the total internal energy and the total volume change by amounts

$$\delta U = \delta m(u_v - u_l), \delta V = \delta m(v_v - v_l). \tag{1.51}$$

According to the first law the heat exchanged with the reservoir is

$$\frac{\delta Q}{\delta m} = (u_v - u_l) + p(v_v - v_l) \equiv l_v, \tag{1.52}$$

where l_v represents the enthalpy of vaporization per unit mass. However, in meteorology l_v is usually called the *latent heat of vaporization*. This latter name stems from the time that one believed that there were two kinds of heat, namely one which one can feel, the sensible heat, and another kind which one cannot feel, the latent heat. Likewise, meteorologists call the turbulent heat flux a sensible heat flux, and the turbulent moisture flux the latent heat flux. Eq. (1.52) can be rewritten as

$$\left(\frac{du}{dv}\right)_T = \left[\frac{l_v}{(v_v - v_l)} - p\right], \tag{1.53}$$

This expression is in a similar form as our starting equation (1.48), and because for this case the pressure p is the saturation vapor pressure e_s we can express its temperature dependency as

$$\frac{de_s}{dT} = \frac{1}{T}\frac{l_v}{(v_v - v_l)}. \tag{1.54}$$

This equation is called the Clausius-Clapeyron equation. Note that the partial derivative is replaced by a total derivative because the saturation pressure depends only on temperature.

If we assume that the specific volume of the liquid water is much smaller than that for the water vapor, $v_l \ll v_v$, and because water vapor is to a good approximation an ideal gas, $e_s v_v = R_v T$, we can rewrite (1.54) as

$$\frac{1}{e_s}\frac{de_s}{dT} \approx \frac{l_v}{R_v T^2}. \tag{1.55}$$

For typical temperature in the atmospheric boundary layer one may use the following approximate form for e_s Stull (1988)

$$e_s = 610.78 \exp\left[\frac{17.2694(T - 273.16)}{T - 35.86}\right] \qquad \text{[Pa]} \ , \tag{1.56}$$

for absolute temperature temperature T [K].

1.4.1 The dependency of the latent heat of vaporization on the temperature

The latent heat release of vaporization (1.52) can be expressed in terms of enthalpy (1.18),

$$l_v = (u_v - u_l) + p(v_v - v_l) = h_v - h_l. \tag{1.57}$$

Differentiating with respect to temperature shows that the latent heat release of vaporization depends on the temperature as follows,

$$\frac{\partial l_v}{\partial T} = \frac{\partial h_v}{\partial T} - \frac{\partial h_l}{\partial T} = c_{pv} - c_{pw}, \tag{1.58}$$

with c_{pv} and c_{pw} according to (1.20) the specific heats for water vapor and liquid water, respectively. For the temperature between 273 and 323 K, the variation of l_v is typically less than 1%.

1.5 Summary

A short summary of basic thermodynamics is presented.

Key elements are:

• If we express the gas law in terms of mass instead of moles, we switch from using the universal gas constants to a specific gas constant which value depends on the molecular weight.

• The dry atmosphere and water vapor can be taken to a good approximation as an ideal gas.

• The state of the atmosphere can be expressed by three state variables, p, v and T, of which two are independent.

• The first law of thermodynamics dictates that energy is conserved.

• For a dry atmosphere a constant-entropy process is also a constant potential temperature process.

• We have derived the Clausius-Clapeyron equation in order to express the saturation vapor pressure as a function of temperature. In the derivation it is crucial that the mixture of liquid water in equilibrium with its vapor is not taken

to behave as an ideal gas. As a consequence, the total internal energy of the mixture depends on the volume.

Chapter 2

Atmospheric thermodynamics

The presence of variable amounts of water in the atmosphere has two important effects. First, it modifies the density of air, and is therefore important to the equation of motion in which the density is major forcing term for the vertical momentum. Second, latent heat release effects play an important role when clouds form of dissipate, which therefore is relevant to the heat budget of atmosphere. The different effects of moisture on heat and density are incorporated in so-called 'temperature' variables, namely the equivalent potential temperature and the virtual (potential) temperature, respectively.

The effect of water vapor and liquid water loading on the density will be discussed. With aid of the thermodynamic laws *conserved variables* can be derived, i.e. variables that are conserved under adiabatic processes regardless of the state of saturation of the air parcel. For instance, for a dry atmosphere the potential temperature is a conserved variable, but in a cloudy atmosphere it is *not* conserved anymore. Instead, for a cloudy atmosphere one may use the equivalent potential temperature or the liquid water potential temperature.

2.1 Moisture variables

In many dutch houses a hygrometer, a thermometer and a barometer are placed on the wall. Some hygrometers, like the hair hygograph, measure the relative humidity by means of a treated human or horse hair. The hair shrinks by about 2.5 per cent of its length when the relative humidity of the atmosphere changes from 100% to zero. In meteorology, one often uses dimensionless measures in terms of the ratio of mass of water to either the mass of dry air, or its ratio to the total mass of dry air and of water. The former is called the mixing ratio, r, and

the latter the specific humidity q,

$$r_k = \frac{m_k}{m_d} \qquad , \qquad q_k = \frac{m_k}{m} \qquad \text{where } k \in v, l, i \tag{2.1}$$

where the indices 'v', 'l', 'i' indicate water vapor, liquid water, water in the ice phase, respectively. Here $m = m_t + m_d$ the total of mass of air including that of total water m_t, $m_t = m_v + m_l + m_i$, and m_d the mass of dry air. The total specific humidity q_t is defined by

$$q_t = q_v + q_l + q_i, \tag{2.2}$$

and analogously for the mixing ratio. Sometimes for q_v and r_v the index 'v' is omitted. The index 's' is often used to denote the water vapor saturation specific humidity q_s.

The specific humidity and the mixing ratio are simply related as:

$$q_v = \frac{r_v}{1 + r_v} \qquad , \qquad r_v = \frac{q_v}{1 - q_v}. \tag{2.3}$$

Whether one uses either the mixing ratio or the specific humidity appears to be a matter of personal preference. Because in the atmosphere both $q_v \ll 1$ and $r_v \ll 1$ we have $q_v \approx r_v$.

Exercise 3. Apply the gas law to water vapor and dry air to express the saturation mixing ratio r_s as a function of the atmospheric pressure ($p = 1018$ hPa) and the water vapor saturation pressure e_s. Use (1.56) and (2.3) to display in one figure r_s and q_s as a function of the temperature.

Exercise 4. Sometimes the spatial coverage of (liquid water) clouds is depicted by showing the cloud liquid water path (W). It is defined as the vertical integral of the specific liquid water content,

$$W = \int_0^{z_{top}} \rho q_l dz. \tag{2.4}$$

Typical numbers for low clouds such as stratocumulus are about 0.150 kg m^{-2}. If the cloud layer is 500 m thick, what is a typical representative value for the liquid water content q_l in the cloud? For the density take $\rho = 1.1 kg m^{-3}$, and use that the liquid water content increases approximately linearly with height.

Background: The liquid water path is a very important quantity for radiative transfer purposes, as the ratio of the liquid water path and the cloud droplet effective radius r_e gives the cloud optical depth $\tau = 3W/(2\rho_l r_e)$. In stratocumulus $r_e \approx 10\mu$, which for this example gives an optical depth $\tau = 22.5$. Because this value corresponds to a mean cloud albedo of about 0.7, the cloud layer has a significant effect on the radiation budget.

We finalize this section by defining two more quantities. First, the dew point temperature T_d, which is the temperature to which air with partial vapor pressure e has to be cooled such that the vapor pressure becomes equal to the saturation vapor pressure,

$$e_s(T_d) = e. \tag{2.5}$$

Second, we note that water vapor can be measured by a wet-bulb psychrometer, which consists of two thermometers, one of which measures the air temperature, the other one has its bulb covered by with a wet (water) muslin wick to give the so-called wet-bulb temperature T_w. Air flows around the wet bulb and if not saturated, water will evaporate until it becomes saturated. The thermodynamic system to be considered is a certain mass of dry air (that has flowed around the bulb) plus water which is evaporated into the air until it reaches saturation. The heat needed for the evaporation is extracted from the air itself. The relation between the two temperatures and the actual specific humidity is

$$T - T_w = \frac{l_v}{c_p}[q_s(T_w) - q_v(T)]. \tag{2.6}$$

2.2 The virtual (potential) temperature

We will derive an expression that incorporates the effect of water vapor and liquid water on the density. Because of the large density of liquid water (ρ_l), which is about 1000 times larger than that of dry air, we may neglect its specific volume ($v_l = V_l/m_l = 1/rho_l$) but, however, not its mass.

The total mass of water in its vapor and liquid phase is $m_v + m_l$, and the mass of dry air is m_d, which determines the total mass $m = m_d + m_v + m_l$ that is contained in a volume $V = V_g + V_l$, where V_g is the volume occupied by the gases. Note that we do not consider water in the ice phase. As $V_l \ll V_g$, $V \approx V_g$, and we can express the density of the mixture ρ as

$$\rho = \frac{m}{V} = \frac{m_d + m_v + m_l}{V}. \tag{2.7}$$

If we compare this density to the density of dry air, ρ_d, and according to the definitions for the specific humidities (2.1) we find

$$\frac{\rho_d}{\rho} = \frac{m_d}{m_d + m_v + m_l} = 1 - q_v - q_l. \tag{2.8}$$

By the gas law we have for the partial pressure $p_d = \rho_d R_d T$ and $e = \rho_v R_v T$. If we neglect the effect of liquid water on the pressure, the total pressure reads

$$p = p_d + e = \rho R_m T = \rho_d R_d T + \rho_v R_v T. \tag{2.9}$$

By (2.8) the gas constant for the mixture R_m can thus be expressed as

$$R_m = (1 - q_v - q_l)R_d + q_v R_v. \tag{2.10}$$

We aim to use the gas constant for dry air R_d rather than the specific gas constant for the mixture R_m. To this end, we can express the gas law in the following from

$$p = \rho R_m T = \rho \left[(1 - q_v - q_l)R_d + q_v R_v\right] T = \rho R_d T_v \tag{2.11}$$

by which we have defined the virtual temperature T_v,

$$T_v = \left[1 - (1 - \frac{1}{\epsilon})q_v - q_l)\right] T, \tag{2.12}$$

with $\epsilon = R_d/R_v \approx 0.622$.

Virtual temperature is the temperature that air of given pressure and density would have if the air were completely free of water. In the absence of liquid water, the virtual temperature is never less than temperature because the mean molecular weight of moist air is never greater than that of dry air. The q_l term in (2.12) tends to diminish the virtual temperature and is sometimes called the *liquid water loading term*. Analogously to (1.36), the *virtual potential temperature* is defined as

$$\theta_v = T_v \left(\frac{p_0}{p}\right)^{\frac{R_d}{c_p}}. \tag{2.13}$$

2.3 The equivalent potential temperature

We have seen that the potential temperature for dry air parcels which are displaced vertically is constant, provided that the process is isentropic. Consider an adiabatically and reversibly rising, moist air parcel. During its ascent the saturation vapor pressure will decrease as the temperature of the environment decreases with height, which is a consequence of the Clausius-Clapeyron equation. At some point the water vapor pressure of the parcel will be equal to its saturation value. If the parcel continues to rise through an increasingly colder atmosphere, liquid water will condense which results in a release of latent heat. This effect of additional heating is included in the *equivalent potential temperature* θ_e, a conserved quantity for isentropic processes that involves phase changes, and is therefore an appropriate quantity when one has to deal with cloudy atmospheres. Its approximate form reads

$$\theta_e \approx \theta \exp\left(\frac{l_v q_v}{c_p T}\right). \tag{2.14}$$

As the argument in the exponential function is sufficiently small, we can further approximate

$$\theta_e \approx \theta + \frac{l_v}{c_p} q_v. \tag{2.15}$$

Similarly, another quantity that is conserved for isentropic processes including phase changes is the *liquid water potential temperature*,

$$\theta_l \approx \theta - \frac{l_v}{c_p} q_l. \tag{2.16}$$

Because $q_t = q_v + q_l$, we have $\theta_l = \theta_e - (l_v/c_p)q_t$. Note that θ_e and θ_l are not conserved anymore when precipitation removes liquid water, or when raindrops evaporate in unsaturated air.

Example

The key ingredients for the derivation of the equivalent potential temperature can be summarized as follows:

1. Consider the total entropy mixed parcel which contains dry air, water vapor and liquid water.

2. Take into account phase changes. This means that latent heat effects must be considered, and that the masses of liquid water and water vapor are variable as an increase in liquid water leads to a similar decrease in water vapor.

3. Use the Clausius-Clapeyron equation.

4. The resulting conservation equation for the entropy of the mixture is long. At this point one may start to make some approximations.

Following step 1, the total entropy of the parcel is

$$S = m_d s_d + m_v s_v + m_l s_l. \tag{2.17}$$

For the change in the entropy we can write

$$dS = d(m_d s_d) + d(m_v s_v) + d(m_l s_l) = m_d ds_d + m_v ds_v + d_v dm_v + m_l ds_l + d_l dm_l, \tag{2.18}$$

where we take the mass of dry air m_d constant. Step 2 involves conservation of total water mass,

$$dm_v = -dm_l. \tag{2.19}$$

The latent heat of vaporization can be introduced into (2.18) by differentiating the first law (1.32) with respect to volume,

$$T\frac{\partial s}{\partial v} = \frac{\partial u}{\partial v} + p. \tag{2.20}$$

For liquid water and water vapor in equilibrium at temperature T and pressure p (2.20) yields,

$$T(s_v - s_l) = u_v - u_l + p(v_v - v_l) = h_v - h_l = l_v. \tag{2.21}$$

Substituting (2.19) and (2.21) into (2.18)gives

$$dS = m_d ds_d + m_v ds_v + m_l ds_l + \frac{l_v}{T} dm_v. \tag{2.22}$$

The entropies for dry air and water vapor can be expressed as

$$ds_d = \frac{c_{pd}}{T} dT - \frac{R_d}{p_d} dp_d, \tag{2.23}$$

$$ds_v = \frac{c_{pv}}{T} dT - \frac{R_v}{e} de = \frac{c_{pv}}{T} dT - \frac{R_v}{e} \frac{de}{dT} dT. \tag{2.24}$$

For liquids and solids the rate of change for any process is given by

$$ds_l = \frac{c_l}{T} dT. \tag{2.25}$$

If we use (2.23), (2.24), and (2.25), we can express the entropy change (2.22) as

$$dS = \frac{l_v}{T} dm_v + (m_l c_l + m_v c_{pv} + m_d c_{pd}) \frac{1}{T} dT - \frac{m_v R_v}{e_s} \frac{de_s}{dT} dT - \frac{m_d R_d}{p_d} dp_d. \tag{2.26}$$

In the last equality we introduced the Clausius-Clapeyron equation thereby applying step 3. If we denote the total mass of the system $m = m_d + m_v + m_l$, use the relation that expresses the temperature dependency of the latent heat of vaporization (1.58), and Clausius-Clapeyron (1.55), then (2.26) can be rewritten as

$$dS = [(m_v + m_l) c_l + m_d c_{pd}] \frac{1}{T} dT + d\left(\frac{l_v m_v}{T}\right) - \frac{m_d R_d}{p_d} dp_d. \tag{2.27}$$

Lastly, this equation can be written in a compact form

$$ds = c_p' d \ln T + d\left(\frac{l_v q_v}{T}\right) - \frac{R_d'}{d} \ln p_d. \tag{2.28}$$

with an effective specific heat $c_p' = (q_t c_l + (1 - q_t) c_{pd})$ and an effective specific gas constant $R_d' = (1 - q_t) R_d$. Note that equation (2.28) is exact.

If we define the potential temperature for dry air,

$$\theta_d = T \left(\frac{p_0}{p_d}\right)^{\frac{R_d'}{c_p'}} \qquad \Longleftrightarrow \qquad c_p' d \ln \theta_d = c_p' d \ln T - R_d' d \ln p_d, \tag{2.29}$$

with p_0 a reference pressure (usually set to 1000 hPa). Note that this is not exactly the same as the potential temperature defined by (1.36), because of the difference $p = p_d + e_s$, and the slightly different specific heat and specific gas constant. By (2.29) we can rewrite (2.28) as

$$ds = d\left(c_p' \ln \theta_d + \frac{l_v q_v}{T}\right) = 0. \tag{2.30}$$

Assume a parcel with temperature T, dry potential temperature θ_d, and a specific humidity q. For isentropic motion, $ds = 0$, and (2.28) can be integrated to obtain the temperature after a vertical displacement. At a sufficiently low pressure all the water vapor will have condensed such that $q_{vf} = 0$, where the subscript 'f' denotes the final state. If we denote $\theta_e = \theta_{df}$ then

$$c_p'\left(\ln \frac{\theta_e}{\theta_d}\right) = \frac{l_v q_v}{T} \qquad \Longleftrightarrow \qquad \theta_e = \theta_d \exp\left(\frac{l_v q_v}{c_p' T}\right). \tag{2.31}$$

If we compare this with the expression (2.14) introduced at the introduction of this session, we see that the latter involves a few implicit assumptions. First, the potential temperature for dry air is replace by the potential temperature (1.36). This means that we neglect the effect of water on the specific heat and the specific gas constant, and that we neglect the effect of the vapor pressure on the total pressure.

Figure 2.1 shows an example of the vertical thermodynamic structure of a stratocumulus cloud deck. These kind of clouds often develop over the oceans in high-pressure systems such as in the descending branch of the Hadley circulation. The boundary layer is usually capped by a well-defined temperature inversion that acts to trap moisture which is evaporated from the surface. As a result horizontally extended cloud fields can develop (1000×1000 km^2). They also do frequently appear above the North Sea. In addition to a weak buoyancy flux from the surface, latent heat release effects and a strong radiative cooling at the top of the cloud layer support the formation of turbulence which tends to make the vertical structure of conserved variables well-mixed. For all quantities shown in the figure a discontinuity occurs across the inversion. The cloud base is located at about 250 m. Above this height the liquid water content increases approximately linearly with height to a maximum value of about 0.8 g/kg. In the boundary layer the temperature decreases with heigth, and the potential temperature and the virtual potential temperature both increase with height. The difference in the two latter quantities is mainly due to the effect of the specific humidity term, $\theta_v = \theta(1 + 0.61 q_v - q_l)$. In the cloud layer, the vertical profiles for conserved quantities like the equivalent potential temperature, the liquid water potential temperature and the total specific humidity deviate slightly from a constant value.

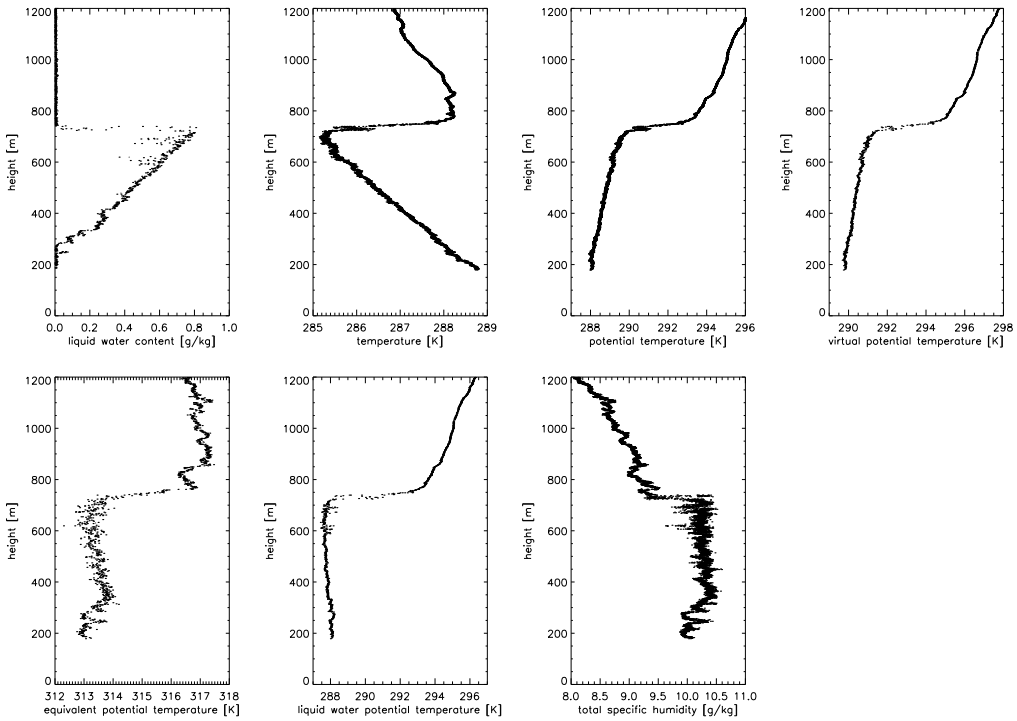

Figure 2.1: Vertical profiles in a stratocumulus-topped boundary layer measured during night-time by an aircraft during flight A209 of the Atlantic Stratocumulus Transition Experiment (ASTEX), 13 June 1992. The figures show the liquid water content q_l, the temperature T, the potential temperature θ, the virtual potential temperature θ_v, the equivalent potential temperature θ_e, the liquid water potential temperature θ_l, and total specific humidity q_t.

2.4 Summary

• We have introduced various variables that are used to give the (relative) water vapor content, like the mixing ratio, the specific humidity, the relative humidity.

• The equivalent potential temperature and the liquid water potential temperatures are conserved for isentropic processes involving phase changes.

Chapter 3

Governing equations for shallow convection in clear and cloudy atmospheres

The state of the atmosphere changes not only by diabatic processes like radiation and precipitation, but also by advection including turbulent motions. The basic approach to derive a simplified set of equations describing turbulent flows involves Reynolds-averaging. This technique splits variables into a mean and a fluctuation part, the latter being associated with the turbulent motions. The turbulent transport of heat, moisture, pollutants and chemical species is then represented by so-called Reynolds-averaged fluxes. In this chapter we will present the governing equations for *shallow* convection. A more elaborate description of the material contained in this chapter can be found in the book 'An introduction to Boundary layer Meteorology', by Stull (1988).

3.1 Governing equations for the mean state and motions in the atmosphere

In addition to the gas law, we will use conservation equations for momentum, heat, moisture and mass. The gas law in terms of the virtual temperature T_v and the density of moist air ρ reads

$$p = \rho R_d T_v. \tag{3.1}$$

We will use the tensor notation so that u_i is the velocity vector in a Cartesian coordinate system x_i with $i \in \{1, 2, 3\}$ such that $\overrightarrow{u} = (u_1, u_2, u_3) \equiv (u, v, w)$ and

$\overrightarrow{x} = (x_1, x_2, x_3) \equiv (x, y, z)$ where z aligned with the gravitational acceleration vector. In addition, δ_{ij} indicates the Kronecker's delta function

$$\delta_{ij} \begin{cases} +1 & \text{for } m = n \\ 0 & \text{for } m \neq n, \end{cases} \tag{3.2}$$

and ϵ_{ijk} the alternating unit tensor (or the Levi-Civita symbol),

$$\epsilon_{ijk} \begin{cases} +1 & \text{for } ijk = 123, 231 \text{ or } 312 \\ -1 & \text{for } ijk = 321, 213 \text{ or } 132 \\ 0 & \text{for any two or more indices alike.} \end{cases} \tag{3.3}$$

The conservation for mass, or the continuity equation, is given by

$$\frac{\partial \rho}{\partial t} + \frac{\partial \rho u_j}{\partial x_j} = 0 \qquad \Longleftrightarrow \qquad \frac{\partial u_j}{\partial x_j} = -\frac{1}{\rho}\frac{d\rho}{dt}, \tag{3.4}$$

and the conservation of momentum reads

$$\frac{du_i}{dt} = -\delta_{i3} g + f \epsilon_{ij3} u_j - \frac{1}{\rho}\frac{\partial p}{\partial x_i} + \frac{1}{\rho}\frac{\partial \tau_{ij}}{\partial x_j}, \tag{3.5}$$

g the acceleration due to the Earth's gravity, and the material derivative

$$\frac{d}{dt} \equiv \frac{\partial}{\partial t} + u_j \frac{\partial}{\partial x_j}. \tag{3.6}$$

The coriolis parameter $f = 2\omega \sin\phi$, where ϕ is the latitude and $\omega = 7.27 \times 10^{-5}$ s^{-1} is the angular velocity of the earth. For a Newtonian fluid, i.e. a fluid for which the viscous stress is linearly dependent on the shear, the viscous stress tensor τ_{ij} is given by

$$\tau_{ij} = \mu \left(\frac{\partial u_i}{\partial x_j} + \frac{\partial u_j}{\partial x_i} \right) + \left(\mu_B - \frac{2}{3}\mu \right) \frac{\partial u_k}{\partial x_k} \delta_{ij} \tag{3.7}$$

where μ_B is the bulk viscosity coefficient (near zero for most gases) and μ is the dynamic viscosity coefficient. If we further assume that the viscosity μ is not a function of position, and that air is incompressible we can express the last term in (3.5) as

$$\frac{1}{\rho}\frac{\partial \tau_{ij}}{\partial x_j} = \nu \frac{\partial^2 u_i}{\partial x_j^2}, \tag{3.8}$$

where the kinematic viscosity ν is defined as the ratio of dynamic viscosity (μ) to the density, $\nu \equiv \mu/\rho$.

The conservation equations for heat (θ) and moisture (q_t) read, respectively,

$$\frac{d\theta}{dt} = \nu_\theta \frac{\partial^2 \theta}{\partial x_j^2} - \frac{1}{\rho c_p}\left(\frac{\partial F_j}{\partial x_j}\right) - \frac{L_p E}{\rho c_p}, \tag{3.9}$$

$$\frac{dq_t}{dt} = \nu_q \frac{\partial^2 q}{\partial x_j^2} + \frac{S_{q_t}}{\rho}, \tag{3.10}$$

with ν_θ the thermal diffusivity and ν_q the molecular diffusivity for water vapor in the air, E represents the mass of water vapor per unit volume per unit time being created by a phase change from liquid or solid, L_p is the latent heat associated with the phase change of E. The values for latent heat at 0°C are $L_v = 2.50 \times 10^6$ J/kg (gas:liquid), $L_f = 3.34 \times 10^5$ J/kg (liquid:solid) and $L_s = 2.83 \times 10^6$ J/kg of water (gas:solid). S_{q_t} is a source/sink function and can represent, for instance, precipitation. Likewise, the conservation equation for an arbitrary chemical species c reads,

$$\frac{dc}{dt} = \nu_c \frac{\partial^2 c}{\partial x_j^2} + S_c \tag{3.11}$$

where S_c represents a loss/gain term due to a chemical reaction.

3.2 Reynolds-averaging rules

A means to separate large-scale (synoptic) fluctuations from turbulent motions is provided by the Reynolds-averaging procedure. Consider a variable a that is split into a mean part ($\overline{A}$) and a turbulent part a', $a = \overline{A} + a'$. If we let c denote an arbitrary constant, then the Reynolds-averaging rules read

$$\begin{aligned}
\overline{cA} &= c\overline{A} \\
\overline{(\overline{A})} &= \overline{A} \\
\overline{(\overline{A}B)} &= \overline{A}\ \overline{B} \\
\overline{A+B} &= \overline{A} + \overline{B} \\
\overline{\left(\frac{dA}{dt}\right)} &= \frac{d\overline{A}}{dt}.
\end{aligned} \tag{3.12}$$

Averaging yields

$$\overline{a} = \overline{(\overline{A} + a')} = \overline{(\overline{A})} + \overline{a'}, \tag{3.13}$$

which can only be equal if

$$\overline{a'} = 0 \quad \Longrightarrow \quad \overline{a} = \overline{A}. \tag{3.14}$$

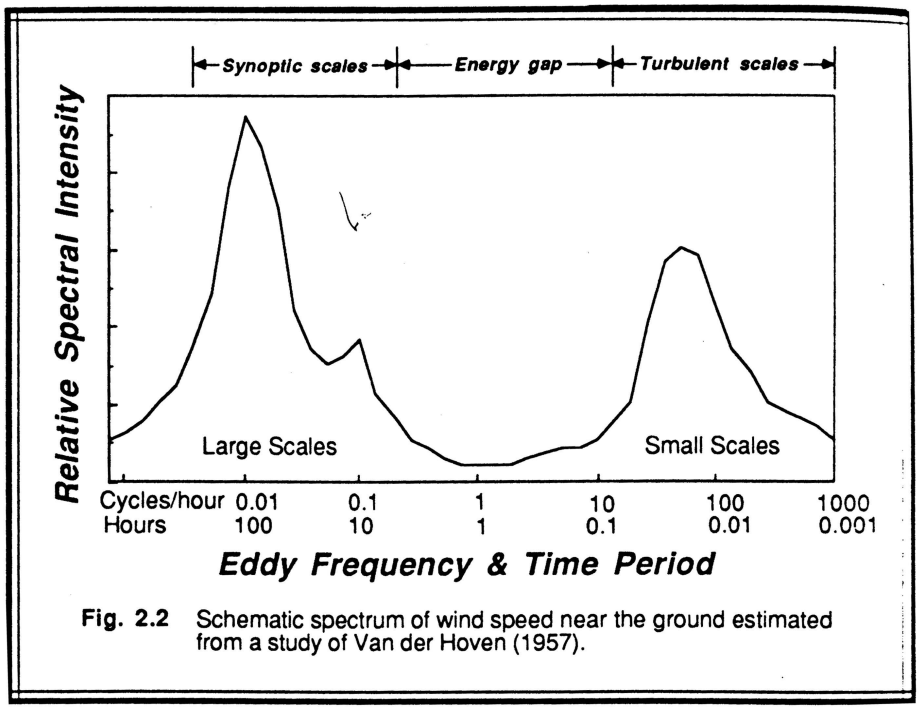

Figure 3.1: Schematic spectrum of wind speed near the ground estimated from a study of Van der Hoven (1957). *Source: Stull (1988)*

Things become less straightforward if we consider multiplications, e.g. $a \cdot b$,

$$\overline{a \cdot b} = \overline{(\overline{A} + a')(\overline{B} + b')} = \overline{A}\ \overline{B} + \overline{a'b'}. \tag{3.15}$$

The Reynolds-averaging approach is valid only for variables that exhibit a clear separation in length scales. In practice, this means that if one makes a Fourier transformation of a quantity, its spectrum is assumed to have a distinct minimum intensity at scales between $\sim$ 1 and $\sim$ 10 km, as illustrated from observations displayed in Figure 3.1. Note that this local minimum is supposed to separate turbulent from synoptic scale fluctuations and is refered to as the *spectral gap*. Therefore, if we apply Reynolds decomposition and the averaging rules (3.12) we tacitly assume the existence a spectral gap. Observations usually show that the amplitude of the vertical velocity fluctuations at scales larger than the boundary-layer depth becomes very small. However, this is often not the case for quantities like temperature, humidity and the horizontal wind velocity components, implying that they do not exhibit a spectral gap.

3.3 Approximations and scaling

3.3.1 The incompressibility approximation

Let us denote U and L as typical velocity and length scales for the boundary layer, c_s the velocity of sound and f is the frequency of any pressure wave that might occur. The density drops out of the continuity equation if the following conditions are satisfied, (1) $U \ll 100$ ms^{-1}, (2) $L \ll 12$ km, (3) $L \ll c_s^2/g$, and (4) $L \ll c_s/f$. For the boundary layer these conditions are usually met which allows to approximate the continuity equation (3.4) as:

$$\frac{\partial u_j}{\partial x_j} = 0. \tag{3.16}$$

This form of the continuity equation states that in shallow convection compressibility effects that are embodied in $d\rho/dt$ can be neglected.

3.3.2 The linearized ideal gas law

In Chapter 2 the virtual temperature was introduced. With aid of the Reynolds-averaged gas law it will be shown that in the vertical momentum equation density fluctuations can be replaced by virtual potential temperature fluctuations.

If we split p, T_v and ρ into a mean and a fluctuating part, and insert this into the gas law (3.1) we obtain,

$$\frac{\overline{p}}{R_d} + \frac{p'}{R_d} = \overline{\rho}\,\overline{T_v} + \overline{\rho}T_v' + \rho'\overline{T_v} + \rho' T_v', \tag{3.17}$$

which after Reynolds averaging yields

$$\frac{\overline{p}}{R_d} = \overline{\rho}\,\overline{T_v} + \overline{\rho' T_v'} \approx \overline{\rho}\,\overline{T_v}, \tag{3.18}$$

which states that the gas law holds in the mean because $\overline{\rho' T_v'} \ll \overline{\rho}\,\overline{T_v}$. In the following this form of the gas law will be used twice. First we subtract it from (3.17),

$$\frac{p'}{R_d} = \overline{\rho}T_v' + \rho'\overline{T_v} + \rho' T_v'. \tag{3.19}$$

Second, we can divide this equation by (3.18)

$$\frac{p'}{\overline{p}} = \frac{\rho'}{\overline{\rho}} + \frac{T_v'}{\overline{T_v}} + \frac{\rho' T_v'}{\overline{\rho}\,\overline{T_v}}. \tag{3.20}$$

The last term on the right-hand side is much smaller than the others and can be neglected. In that case we arrive at the *linearized perturbation ideal gas law*:

$$\frac{p'}{\overline{p}} = \frac{\rho'}{\overline{\rho}} + \frac{T_v'}{\overline{T_v}}. \tag{3.21}$$

In the boundary layer the pressure fluctuation term is very small in comparison to $T_v'/\overline{T_v}$. In the *shallow convection approximation* the pressure effect in (3.21) is therefore neglected:

$$\frac{\rho'}{\overline{\rho}} = -\frac{T_v'}{\overline{T_v}}. \tag{3.22}$$

By the definition of the virtual potential temperature (2.13) we can also write

$$\frac{\rho'}{\overline{\rho}} = -\frac{\theta_v'}{\overline{\theta_v}}. \tag{3.23}$$

In a model it is not really necessary to use θ_v' fluctuations instead of ρ'. The advantage of θ_v arises from an observational point of view as this quantity requires the measurement of temperature and moisture content (and liquid water in case of a cloudy atmosphere) which is less difficult than measuring the density.

3.3.3 The Boussinesq approximation

Let us consider the vertical component ($i = 3$) of the conservation of momentum equation (3.5):

$$\frac{dw}{dt} = -g - \frac{1}{\rho}\frac{\partial p}{\partial z} + \nu\frac{\partial^2 w}{\partial x_j^2}, \tag{3.24}$$

If we (1) expand w, p and ρ into a mean and turbulent part, (2) multiply by $((\overline{\rho} + \rho')/\overline{\rho})$ and (3) assume that the mean state is in a hydrostatic equilibrium ($\partial\overline{p}/\partial z = -\overline{\rho}g$), we obtain

$$\left(1 + \frac{\rho'}{\overline{\rho}}\right)\frac{dw'}{dt} = -\frac{\rho'}{\overline{\rho}}g - \frac{1}{\overline{\rho}}\frac{\partial p'}{\partial z} + \nu\frac{\partial^2 w'}{\partial x_j^2}, \tag{3.25}$$

where we assume that the viscosity is constant, and we use that the large-scale vertical advection is typically much smaller than the fluctuations of the vertical velocity, $\overline{w} \ll w'$. The *Boussinesq approximation* makes use of the fact that $\rho'/\overline{\rho}$ is on the order 3.33×10^{-3} such that $1 + \rho'/\overline{\rho} \approx 1$, from which follows

$$\frac{dw'}{dt} = -\frac{\rho'}{\overline{\rho}}g - \frac{1}{\overline{\rho}}\frac{\partial p'}{\partial z} + \nu\frac{\partial^2 w'}{\partial x_j^2}. \tag{3.26}$$

Or by (3.23) we can also write

$$\frac{dw'}{dt} = \frac{\theta_v'}{\overline{\theta_v}} g - \frac{1}{\overline{\rho}} \frac{\partial p'}{\partial z} + \nu \frac{\partial^2 w'}{\partial x_j^2}. \tag{3.27}$$

The Boussinesq-approximated form of the vertical wind velocity fluctuation equation can be used to derive prognostic equations for higher-order moments like the turbulent kinetic energy or vertical fluxes.

In summary, the derivation of the prognostic equation (3.27) for the vertical velocity fluctuation w' follows from Reynolds-averaging the gas law and the vertical momentum equation. The major assumptions made are that we effectively neglect the role of pressure perturbations on the density in the linearized gas law, and that the mean state of the boundary layer is in a hydrostatic equilibrium.

3.3.4 Reynolds-averaged equations

As is clear from (3.15) Reynolds-averaging of a multiplication $\overline{a \cdot b}$ leads to two terms one of which represents a correlation term of the fluctuations $\overline{a'b'}$. For example, the Reynolds-averaged momentum equation reads

$$\frac{\partial \overline{u_i}}{\partial t} + \overline{u_j} \frac{\partial \overline{u_i}}{\partial x_j} = -\delta_{i3} g + f \epsilon_{ij3} \overline{u_j} - \frac{1}{\overline{\rho}} \frac{\partial \overline{p}}{\partial x_i} + \nu \frac{\partial^2 \overline{u_i}}{\partial x_j^2} - \frac{\partial \overline{u_i' u_j'}}{\partial x_j}, \tag{3.28}$$

and similar correlation terms of perturbations arise for the conservation equations for heat, moisture and scalars. So the implication of Reynolds-averaging is that if we want to predict the evolution of the mean state of the atmosphere we have to consider the effect of turbulence.

3.3.5 Reynolds number

The Reynolds number Re gives the ratio of inertial to viscous forcings,

$$Re = UL/\nu \tag{3.29}$$

where U and L are typical velocity and length scales. Since for air $\nu \approx 1.5 \times 10^5$ $\mathrm{m^2 s^{-1}}$, and if we take typical scaling values $U = 5$ $\mathrm{ms^{-1}}$ and $L = 1000$m, we find that $Re = 3 \times 10^6$. If we apply a scaling analysis to (3.28), it then follows that the term including the viscosity is a factor Re smaller than the other terms. Therefore, this term can be neglected, except in the lowers few centimeters of the surface. Likewise, we can neglect the diffusion terms in the conservation equations for heat, moisture and chemical species.

3.4 Summary of approximated governing equations for mean quantities

$$\overline{p} = \overline{\rho} R_d \overline{T_v} \tag{3.30}$$

$$\frac{\partial \overline{u_j}}{\partial x_j} = 0 \tag{3.31}$$

$$\frac{\partial \overline{u}}{\partial t} + \overline{u_j}\frac{\partial \overline{u}}{\partial x_j} = -\frac{1}{\overline{\rho}}\frac{\partial \overline{p}}{\partial x} + f\overline{v} - \frac{\partial \overline{u_j' u'}}{\partial x_j} \tag{3.32}$$

$$\frac{\partial \overline{v}}{\partial t} + \overline{u_j}\frac{\partial \overline{v}}{\partial x_j} = -\frac{1}{\overline{\rho}}\frac{\partial \overline{p}}{\partial y} - f\overline{u} - \frac{\partial \overline{u_j' v'}}{\partial x_j} \tag{3.33}$$

$$\frac{\partial \overline{\theta}}{\partial t} + \overline{u_j}\frac{\partial \overline{\theta}}{\partial x_j} = -\frac{1}{\overline{\rho} c_p} L_p E - \frac{1}{\overline{\rho} c_p}\frac{\partial \overline{F_j}}{\partial x_j} - \frac{\partial \overline{u_j' \theta'}}{\partial x_j} \tag{3.34}$$

$$\frac{\partial \overline{q_t}}{\partial t} + \overline{u_j}\frac{\partial \overline{q_t}}{\partial x_j} = +\frac{S_{q_t}}{\overline{\rho}} - \frac{\partial \overline{u_j' q_t'}}{\partial x_j} \tag{3.35}$$

$$\frac{\partial \overline{c}}{\partial t} + \overline{u_j}\frac{\partial \overline{c}}{\partial x_j} = +S_c - \frac{\partial \overline{u_j' c'}}{\partial x_j} \tag{3.36}$$

Because the liquid water potential temperature is conserved for isentropic (reversible) processes in which condensation/evaporation of cloud liquid water occurs this quantity is more convenient to use than θ. In particular, the Reynolds-averaged form of the liquid water potential temperature equation reads

$$\frac{\partial \overline{\theta_l}}{\partial t} + \overline{u_j}\frac{\partial \overline{\theta_l}}{\partial x_j} = -\frac{1}{\overline{\rho} c_p}\frac{\partial \overline{F_j}}{\partial x_j} - \frac{\partial \overline{u_j' \theta_l'}}{\partial x_j}. \tag{3.37}$$

By replacing every θ_l occurence by θ_e we obtain an identical entropy conservation equation in terms of the equivalent potential temperature. In the entropy equation the effect of latent heat release is incorporated in θ_l, and comparison to the heat equation (3.34) shows that it does not need to be included by a separate term.

3.5 Governing equations for second-order moments

One can derive a large set of prognostic equations for the mean of any arbitrary second-order moment $\overline{a'b'}$, for instance the vertical velocity variance $\overline{w'^2}$ or the

	$q_v = 0$	$q_v > 0$, $q_l = 0$	$q_l > 0$
gas law	T	T_v	T_v
conservation of momentum	θ	θ_v	θ_v
conservation of heat/entropy	θ	θ	θ_l or θ_e

Figure 3.2: Summary of temperature variables. The columns show the following conditions: no moisture ($q_v = 0$), moisture but no liquid water ($q_v > 0, q_l = 0$), or the presence of liquid water clouds $q_l > 0$, and the rows the equations for which the temperature variables are appropriate.

turbulent heat flux $\overline{u_i'\theta'}$. The prognostic equation for the vertical velocity variance $\overline{u_i'u_i'}$ is given by,

$$\frac{\partial \overline{u_i'^2}}{\partial t} + \overline{u_j}\frac{\partial \overline{u_i'^2}}{\partial x_j} = 2\delta_{i3}\frac{g}{\overline{\theta_v}}\overline{u_i'\theta_v'} - 2\overline{u_i'u_j'}\frac{\partial \overline{u_i}}{\partial x_j} - \frac{\partial \overline{u_j'u_i'^2}}{\partial x_j} - \frac{2}{\overline{\rho}}\frac{\partial \overline{u_i'p'}}{\partial x_i} - 2\epsilon. \tag{3.38}$$

The prognostic equation for the flux $\overline{w'\psi'}$ reads,

$$\begin{aligned}\frac{\partial \overline{u_i'\psi'}}{\partial t} + \overline{u_j}\frac{\partial \overline{u_i'\psi'}}{\partial x_j} = &-\overline{u_j'\psi'}\frac{\partial \overline{u_i}}{\partial x_j} - \overline{u_i'u_j'}\frac{\partial \overline{\psi}}{\partial x_j} - \frac{\partial \overline{u_i'u_j'\psi'}}{\partial x_j} + \delta_{i3}\frac{g}{\overline{\theta_v}}\overline{\psi'\theta_v'} \\ &+ f\epsilon_{ij3}\overline{u_j'\psi'} - \frac{1}{\overline{\rho}}\overline{\left(\psi'\frac{\partial p'}{\partial x_i}\right)} + \nu_\psi\frac{\partial^2 \overline{u_i'\psi'}}{\partial x_j^2} - 2\nu_\psi\overline{\left(\frac{\partial u_i'}{\partial x_j}\right)\left(\frac{\partial \psi'}{\partial x_j}\right)}\end{aligned} \tag{3.39}$$

where $\psi \in \{\theta, q_t, c\}$ and we assumed no source terms ($S_\psi = 0$) and no radiation. The prognostic variance equation for ψ reads

$$\frac{\partial \overline{\psi'^2}}{\partial t} + \overline{u_j}\frac{\partial \overline{\psi'^2}}{\partial x_j} = -2\overline{u_j'\psi'}\frac{\partial \overline{\psi}}{\partial x_j} - \frac{\partial \overline{u_j'\psi'\psi'}}{\partial x_j} - 2\nu_\psi\overline{\left(\frac{\partial \psi'}{\partial x_j}\right)^2} \tag{3.40}$$

3.6 Summary

Figure 3.2 summarizes the temperature variables and three equations discussed in Chapters 1-3.

Part II - Cloud dynamics

Chapter 4

Introduction

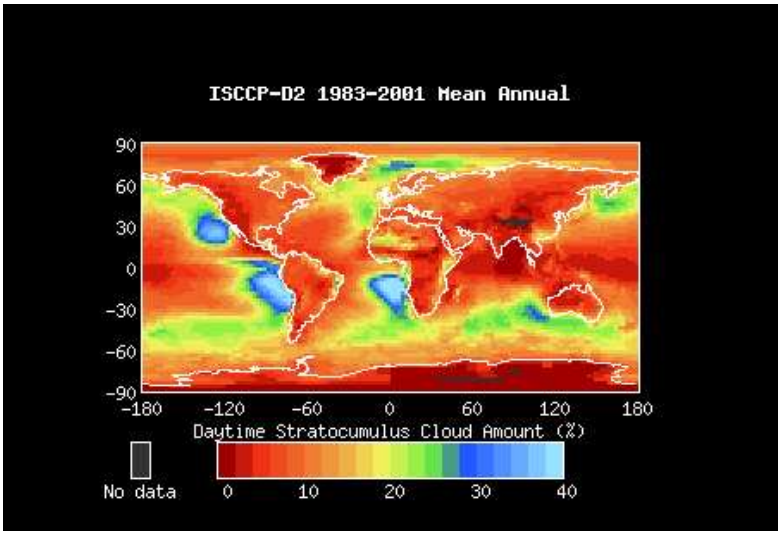

Figure 4.1: The daytime global stratocumulus amount. *Source: The International Satellite Cloud Climatology Project (ISCCP), http://isccp.giss.nasa.gov/.*

Stratus, stratocumulus and shallow cumulus are all classified as boundary layer clouds. Stratus and stratocumulus are layered clouds having cloud fractions close to unity. Shallow cumulus can be characterized by its broken structure and small cloud fraction. Figure 4.1 shows that there is a very persistent presence of stratocumulus clouds in the subtropical areas west of the American continent and Africa. The presence of stratocumulus in the subtropics can be understood by considering the mean flow pattern in subtropics (see Figure 4.2). Due to the

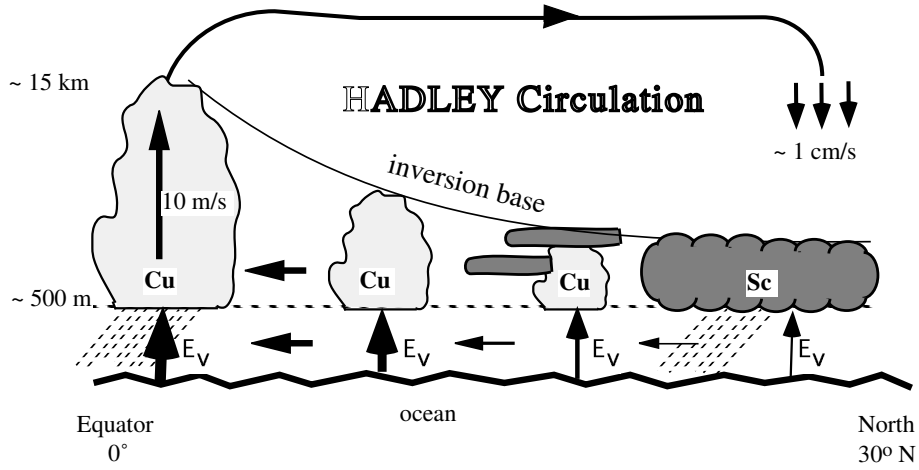

Figure 4.2: Schematic cross section through the trades and ITCZ illustrating the circulation and moistening of the subcloud layer and cloud layer. 'E_v' indicates the surface moisture flux, and 'sc' and 'cu' denote stratocumulus and cumulus clouds, respectively.

large-scale subsidence in the descending branch of the Hadley circulation the observed boundary layers in the subtropical regions are usually relatively shallow. The boundary layers are capped by a stable temperature inversion that acts to trap the moisture that is evaporated from the sea surface. This supports the formation and maintenance of horizontally extended stratocumulus fields. The surface winds transport air from the subtropics towards the equator. Along this path the sea surface temperature gradually increases and a subsequent transition from stratocumulus to cumulus takes place.

Figure 4.3 shows a selection of observations of the downwelling shortwave radiation under a stratocumulus cloud deck for which the cosine of the solar zenith angle θ_0 has a fixed value, $\mu_0 = \cos\theta_0 = 0.95$. It is clear that stratocumulus clouds can reflect back to space a significant part of the downwelling shortwave radiation. The line shows modeling results obtained with a δ-Eddington model, which will be explained in detail later in this course.

Stratus is also frequently observed in the Arctic region. The formal distinction between stratus and stratocumulus is the cloud optical thickness (τ), where $\tau > 23$ ($\tau < 23$) defines stratus (stratocumulus). However, in practice this definition is rarely strictly applied and in the scientific literature it is not rare to find that a cloud type is called stratus instead of stratocumulus, and vice versa. In particular during the dark winter period Arctic stratus has a strong net warming effect

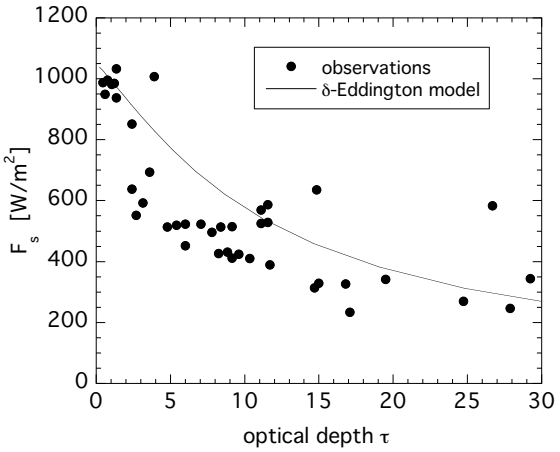

Figure 4.3: The downward short-wave irradiance around solar noon ($\mu_0 = 0.95$) at the surface as a function of optical depth. The dots indicate observations on San Nicolas island and the line results from calculations with a δ-Eddington model. In the model the downwelling shortwave radiation at cloud top was 1100 Wm^{-2}, and the magnitude of the sea surface albedo was 0.05.

due to its emission of longwave radiation. Figure 4.4 displays observations at the SHEBA (Surface Heat and Energy Balance of the Arctic Ocean) ice camp during the Arctic spring. It clearly shows that the net longwave radiation at the surface increases sharply by an amount of about 60 Wm^{-2} during the presence of a cloud layer extending to the surface (fog). Note that the figure shows the *liquid* water path while the temperature during the observations was below freezing, which implies that the cloud must have consisted of *supercooled* liquid water. The increase in the downwelling longwave radiation is due to the presence of cloud water. Stratus and stratocumulus are optically thick and emit radiation as a black body as opposed to a clear atmosphere which emits longwave radiation as a grey body. As a consequence, more infrared radiation is emitted downwards from the cloud top than is received from the atmosphere above, as is illustrated from aircraft observations shown in Figure 4.5. The largest jump in the downward longwave radiation takes place in a shallow layer of several tens of meters thick near the cloud top. In this layer local radiative cooling rates exceeding more than 8 K/hour are not exceptional. It causes radiatively cooled air parcels to sink downwards, thereby redistributing the colder temperatures throughout the cloud mixed layer. There is also a small jump at cloud base which leads to warming.

The radiative cooling of the stratocumulus cloud top generates turbulence that causes conserved variables such as the liquid water potential temperature

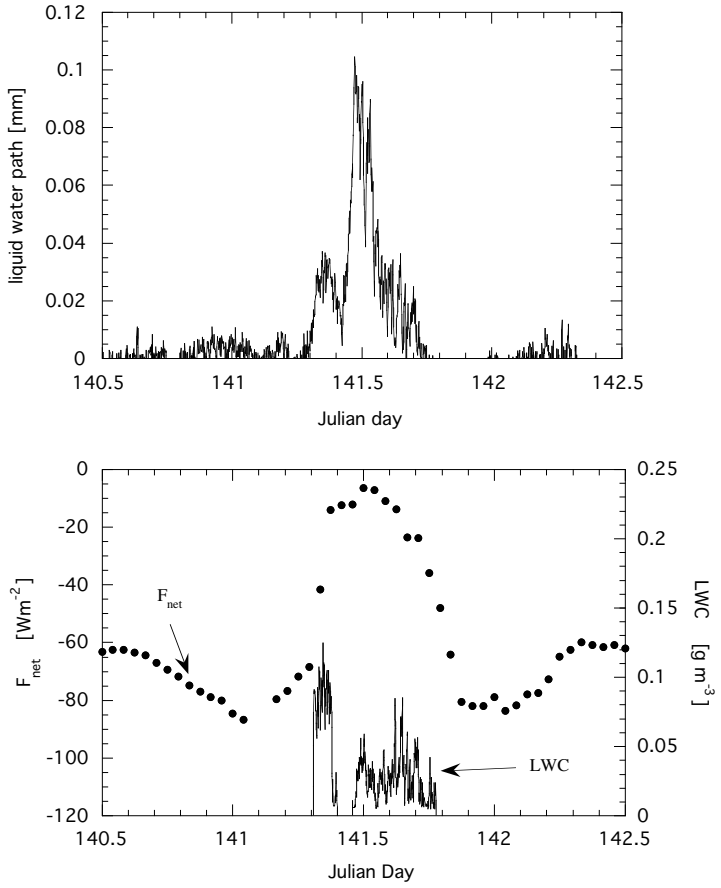

Figure 4.4: Time series of the liquid water path (upper panel) and the net longwave radiation and liquid water content in fog at 2 m above the surface (lower panel). The liquid water path data were obtained with a microwave radiometer and were kindly provided by Dr. J. Liljegren. The measurements were made from 20 to 22 May 1998 (Julian day 140 to 142) at the SHEBA ice camp (76°N, 166°W)

.

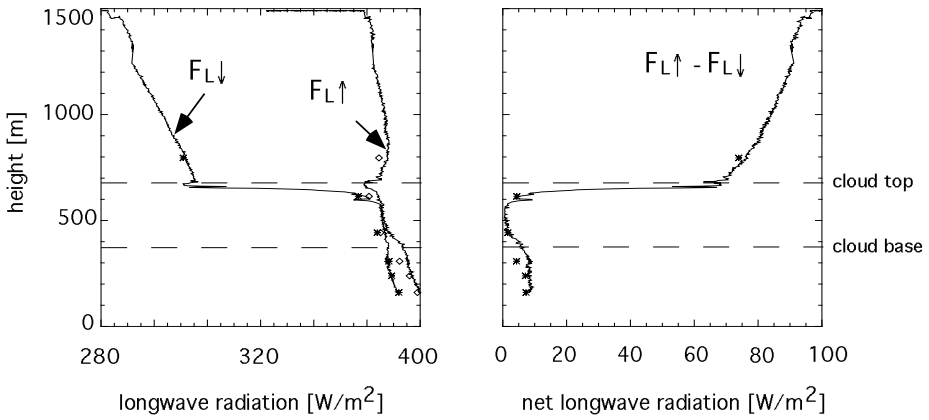

Figure 4.5: The observed upward and downward longwave radiation (left panel) and the net longwave radiation (right panel, same vertical scale as right panel) as a function of height in a stratocumulus-topped boundary layer during ASTEX. The asterisks '$*$' and the diamonds '$\Diamond$' represent mean values during a horizontal aircraft leg ($\pm$ 60 km), and the line indicates results from a slant profile.

and the total specific humidity to become vertically well mixed (see Figure 4.6 for a schematic illustration). From the cloud base to the cloud top the total water specific humidity exceeds the saturation value, i.e. $q_t > q_{sat}$, and due to latent heat release effects the virtual potential temperature approximately follows the wet-adiabatic lapse rate. The cloud top is capped by a strong stable inversion layer in which the temperature can increase by more than $10 \sim 15$°C over a vertical distance of less than 50 m.

During daytime, a significant amount of solar radiation is absorbed by the cloud layer. The solar absorption extends deeply into the cloud layer. As a result, the cloud layer can get warmer more rapidly than the subcloud layer, causing a very small virtual potential temperature jump near the cloud base. In that case the cloud layer becomes stably stratified with respect to the subcloud layer, and the transport of heat and moisture into the stratocumulus cloud by convective eddies driven from the surface is effectively reduced and sometimes even cut off. Radiative cooling will maintain the generation of convection from the cloud top, which results in two well-mixed turbulent layers that are *decoupled* and only interact weakly. Decoupling may lead to a breakup of the cloud because, firstly, solar radiative absorption will cause evaporation of cloud liquid water, and secondly, the cloud layer will dry out if entrainment of dry air at the cloud top continues while the moisture supply at the cloud base by the surface-driven eddies is reduced significantly. Even if these two processes do not lead to a full dissipation of the

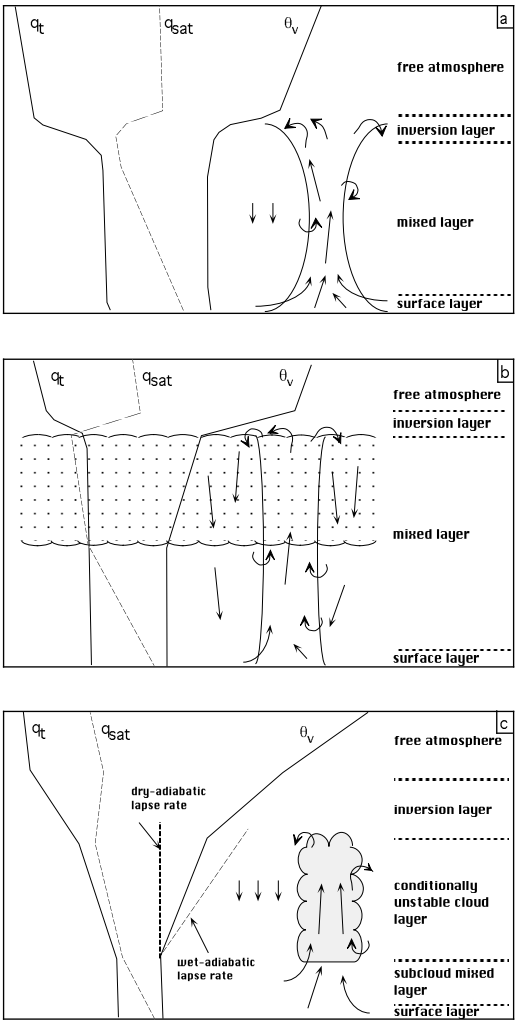

Figure 4.6: Schematic of typical mean profiles for the total specific humidity q_t, the saturation specific humidity q_{sat} and the virtual potential temperature θ_v in a) the clear convective boundary layer, b) stratocumulus and c) cumulus.

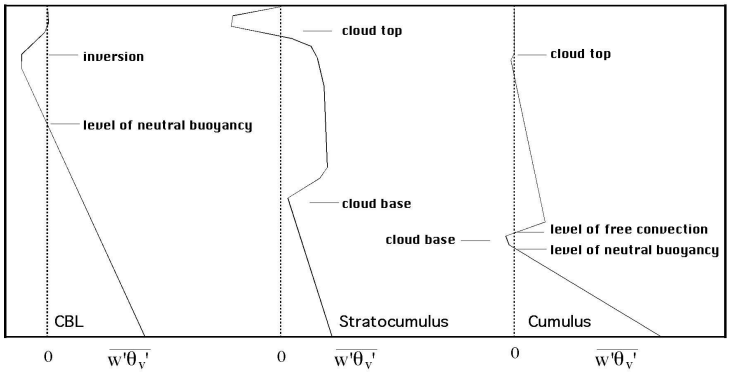

Figure 4.7: Schematic of typical buoyancy flux ($g/\theta_0 \overline{w'\theta'_v}$) profiles in the clear convective boundary layer (left), stratocumulus (middle), and cumulus (right).

cloud layer, they will at least cause a change in the cloud structure. Because of the diurnal cycle of the sun, the cloud amount and cloud fraction will be maximal before and near sunrise while the minimal cloudiness occurs around local noon. Other mechanisms that can cause a temperature jump near cloud base are evaporation of drizzle below cloud base and the subsequent cooling of the subcloud layer.

The subcloud layer of a cumulus-topped boundary layer is also vertically well-mixed. This does not apply to the cloud layer in which the virtual potential temperature profile is in between the dry and the wet-adiabatic lapse rate. Note that in the cloud layer the mean specific humidity is lower than the saturation value ($q_t < q_{sat}$).

Typical examples of vertical profiles for the buoyancy fluxes are displayed in Figure 4.7. In the clear convective boundary the buoyancy flux is approximately linear with height, and the minimum value at the boundary-layer top is due to the downward turbulent mixing (entrainment) of warm air from above the inversion layer. In stratocumulus the longwave radiative cooling explains the sharp jump in the buoyancy flux profile near the cloud top as the cooling produces cold air parcels that sink downwards. The sharp increase in the buoyancy flux that occurs near the cloud base is resulting from latent heat release by condensation of cloud liquid water. Thus both latent heat release effects and longwave radiative cooling act to generate a positive buoyancy flux in the cloud layer. The minimum flux at the cloud top is also due to the entrainment of warm air from above the inversion. In the case of cumulus convection, the buoyancy flux is negative near the top of the subcloud layer. At these levels only the strongest thermals that have sufficient upward momentum can rise through and become saturated. Above this level

the release of latent heat causes the virtual potential temperature difference with respect to the environment to become positive again.

An accurate representation of boundary-layer clouds in large-scale models is problematic. This can be clearly illustrated from a comparison of ECMWF Re-Analysis (ERA) data to observations. The ERA project has produced a new 15 year data set of assimilated data for the period 1979 to 1993. ERA was produced using the ECMWF Integrated Forecasting System (IFS), that contains both the model and the analysis part of the data assimilation system. The ERA data can thus be considered as the best estimate available of the state of the atmosphere for a given time. Figure 4.8 shows the monthly mean diurnal variation of the vertically integrated liquid water content (the liquid water path (LWP)) from stratocumulus observations collected during July 1987 off the coast of California, in addition to monthly-mean ERA results for July 1987, and the average for five subsequent July periods between 1985 and 1989. The overall picture is of a cloud layer that progressively thins during the late morning into the afternoon, and thickens again during the evening. The model strongly underestimates the amount of stratocumululs. This is particularly striking when we compare the peak values of the LWP: about 150 g m^{-2} for the observations and about 20 g m^{-2} for the model in July 1987. The 5 year mean values for ERA are even lower than the July 1987 values.

The effects of an underestimation of the stratocumulus cloud deck has a dramatic effect on the prediction of the sea surface temperature (SST). For example, the SST off the coast of Peru can obtain a warm bias of about 5 K if the stratocumulus amount is underestimated (Ma et al., 1996). This leads to too much solar radiation reaching the surface. This deficiency is in particular relevant for the simulation and the prediction of the El Nino - Southern Oscillation (ENSO).

In the following we will discuss the dynamics of stratocumulus and cumulus clouds. The set-up will be based on the schematic shown in Figure 4. The physical processes in boundary layer clouds will be illustrated mainly from observations and results from Large-Eddy Simulation (LES) models. An LES model is a numerical tool that can solve the turbulence field in clear and cloudy atmospheric boundary layers. The results obtained from observations and LES have provided very much insight of the turbulence and microphysical structure in boundary-layer clouds. This knowledge can be used to design parameterization schemes for the computation of the turbulent transport of heat and moisture in cloud-topped boundary layers. In general circulation models (GCMs) this is a necessity because the turbulent eddies are not resolved by the coarse grid resolution in current GCMs.

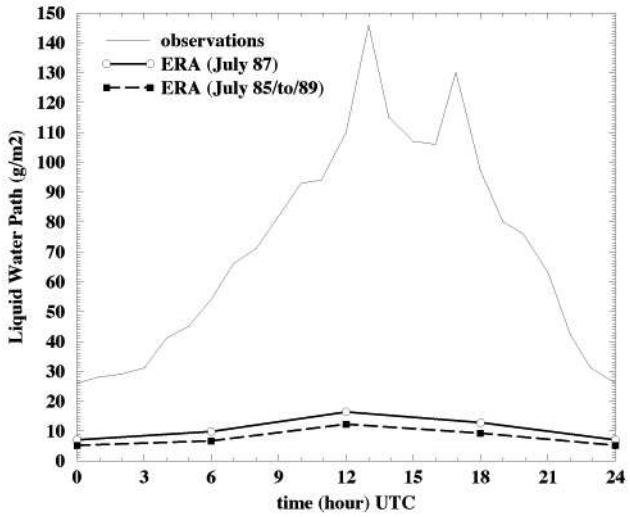

Figure 4.8: Mean diurnal variation of liquid water path: FIRE I observations from 1 to 19 July 1987 (thin line), July 1987 of ERA (thick full line) and July 1985/86/87/88/89 of ERA (dashed line) Duynkerke and Teixeira (2001).

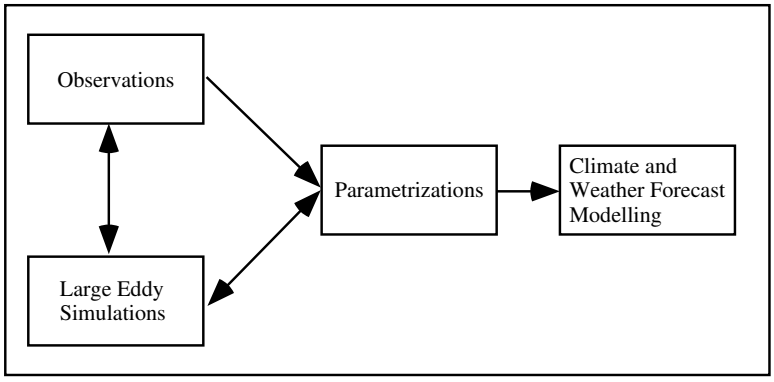

Figure 4.9:

Chapter 5

Stratocumulus clouds

The formation and maintenance of stratocumulus is supported by large-scale subsidence nearby a high pressure system and the input of sufficient moisture from the surface. However, due to turbulent motions at the top of the cloud relatively warm and dry air from above the capping inversion is entrained and subsequently mixed into the cloud layer. It will be explained that the entrainment rate is crucial for understanding the evolution of the stratocumulus-topped boundary layer.

Most of the topics contained in this chapter are also discussed, though with less mathematical details, in Chapter 7 of the book 'The atmospheric boundary layer' by Garratt (1994).

5.1 Turbulent transport in stratocumulus clouds

A typical feature of the clear convective and the nocturnal stratocumulus-topped boundary layer is that conserved variables are approximately constant with height. If the vertical gradient of any mean variable $\psi \in \{q_t, \theta_l, c\}$ does not change with time we can write

$$\frac{\partial}{\partial z}\left(\frac{\partial \overline{\psi}}{\partial t}\right) = 0, \tag{5.1}$$

a situation that is refered to as a *quasi-steady state*. Eq. (5.1) has a direct consequence for the shape of the vertical flux profiles. Let us consider a boundary layer that is horizontally homogeneous ($\partial/\partial x_i(\overline{u_i'\chi'}) = 0$ for $i = 1, 2$) and assume that there is neither mean advection nor radiation. In that case the tendency of $\overline{\psi}$ will be determined by a change with height of the vertical turbulent flux,

$$\frac{\partial \overline{\psi}}{\partial t} = -\frac{\partial \overline{w'\psi'}}{\partial z}, \tag{5.2}$$

and by Eq. (5.1)

$$\frac{\partial}{\partial z}\left(\frac{\partial \overline{\psi}}{\partial t}\right) = -\frac{\partial^2 \overline{w'\psi'}}{\partial z^2} = 0, \tag{5.3}$$

which implies that the vertical gradient of the flux is constant,

$$\frac{\partial \overline{w'\psi'}}{\partial z} = \text{constant} \qquad \Longrightarrow \qquad \overline{w'\psi'} = \overline{w'\psi'}_0(1 - z/z_i) + \overline{w'\psi'}_T z/z_i. \tag{5.4}$$

with z_i the boundary layer height and the indices '0' and 'T' indicating the surface and top values for the flux, respectively. For an infinitesimally thin inversion layer the flux at the boundary layer top can be expressed as

$$\overline{w'\psi'}_T = -w_e \Delta\overline{\psi}, \tag{5.5}$$

with $\Delta\overline{\psi}$ the jump across the inversion, and w_e the entrainment velocity. The latter gives the rate with which the boundary layer height grows with time by the turbulent mixing of free atmospheric air into the boundary layer,

$$\frac{dz_i}{dt} = w_e + \overline{w}, \tag{5.6}$$

with $\overline{w}$ the large-scale velocity. Thus, the surface and entrainment fluxes of heat and moisture determine the temporal evolution of a convective boundary layer. The surface fluxes can be computed by using relations such as given by Monin-Obukhov similarity theory. By contrast, there are currently no scaling relations available that accurately predict the entrainment rate in stratocumulus clouds.

5.2 The mixed-layer model

A mixed-layer model assumes a quasi-steady state boundary layer and includes the effect of radiation or precipitation. The model consists of just three equations and is therefore a very powerful tool to understand the dynamics of stratocumulus. The details of the model that is discussed in this section are adapted from Nicholls (1984), who presents the mixed layer model with θ_e as entropy variable. The model described here uses θ_l and q_t as conserved variables. For simplicity we assume that the effect of moisture and liquid water on c_p and L_v can be neglected. Figure 5.1 shows the typical variation of θ_l and q_l to illustrate certain significant levels, labelled 0 to 4. Cloud top and cloud base are assumed to lie between levels 3 and 4, and 1 and 2, respectively so that levels 2 and 3 are entirely within cloud while the others lie entirely outside.

In summary: levels 0-3 lie within the mixed layer; levels 2 and 3 lie within the cloud layer; and levels 0 and 1 lie within the subcloud layer. Since levels 1 and 2

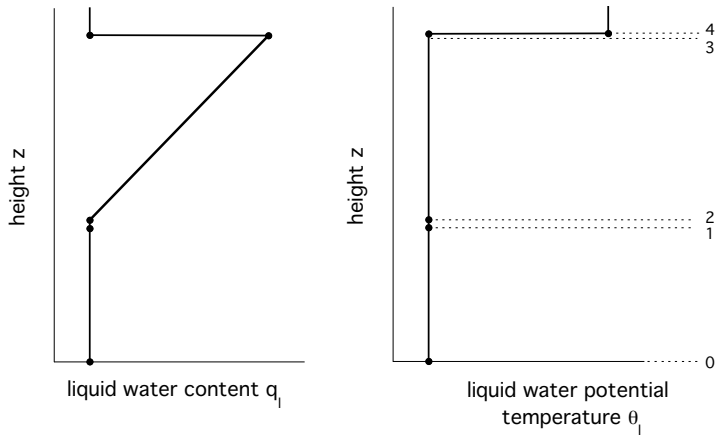

Figure 5.1: Schematic diagram showing idealized q_l and θ_l profiles with significant level notation.

are very close together and within the mixed layer, no flux divergence of conserved variables may occur between them.

At level 3, entirely within the cloud, the turbulent fluxes are assumed to be related to the jumps in variables between levels 3 and 4 according to the flux-jump relation (5.5). Since these two levels also have a negligible height separation, no radiative flux divergence is allowed between them, i.e. all the radiative heating and cooling occurs within the cloud. This is prescribed at additional levels within the cloud layer.

The rates of change of conserved variables within the mixed layer may then be expressed as

$$\frac{d\overline{q_t}}{dt} = -\frac{\partial \overline{w'q_t'}}{\partial z}, \tag{5.7}$$

and

$$\frac{d\overline{\theta_l}}{dt} = -\frac{\partial \overline{w'\theta_l'}}{\partial z} - \frac{\partial F}{\partial z}, \tag{5.8}$$

so it is implicitly assumed that mean horizontal gradients are small. The net radiation flux F is defined by

$$F = \frac{1}{\overline{\rho} c_p}(L\uparrow - L\downarrow + S\uparrow - S\downarrow) + F_0 \tag{5.9}$$

with L and S denoting the longwave and shortwave radiation, respectively. F_0 is a height-independent reference value chosen for convenience to make F zero in the subcloud layer since only the flux divergence within the cloud layer is of

importance here, rather than the absolute value. We assume that there is no precipitation.

As the tendencies for $\overline{q_t}$ and $\overline{\theta_l}$ must be independent of height within the mixed layer, integrating Eqs. (5.7) and (5.8) between levels 0 and 3 yields

$$\frac{d\overline{q_t}}{dt} = \frac{w_e \Delta \overline{q_t} + \overline{w'q'_{t0}}}{z_i}, \tag{5.10}$$

and

$$\frac{d\overline{\theta_l}}{dt} = \frac{w_e \Delta \overline{\theta_l} + \overline{w'\theta'_{l0}}}{z_i} + F_3 - F_0, \tag{5.11}$$

where we used the entrainment-jump relation (5.5) and for the mixed-layer depth z_i the height of level 3, $z_3 = z_i$.

Vertically integrating Eq. (5.7) from level 0 to some arbitrary level p (such that $z_p \leq z_i$) and substituting Eq. (5.10) gives

$$\overline{w'q'_{tp}} = \overline{w'q'_t}(z = z_p) = \left(1 - \frac{z}{z_i}\right) \overline{w'q'_{t0}} - \left(\frac{z}{z_i}\right) w_e \Delta \overline{q_t}, \tag{5.12}$$

and likewise

$$\overline{w'\theta'_{lp}} = \left(1 - \frac{z}{z_i}\right) \left(\overline{w'\theta'_{l0}} + F_0\right) + \frac{z}{z_i} \left(F_3 - w_e \Delta \overline{\theta_l}\right) - F_p. \tag{5.13}$$

Turbulent transfer is assumed to be extinguished at level 4 by the strong stable stratification and the turbulent fluxes are therefore set to zero. Note in the absence of sources and sinks the flux equation for a passive scalar c is given by

$$\overline{w'c'}_p = \left(1 - \frac{z}{z_i}\right) \overline{w'c'}_0 - \left(\frac{z}{z_i}\right) w_e \Delta \overline{c}. \tag{5.14}$$

The mixed-layer model is thus given by the prognostic equation for the boundary layer height (5.6) and by the two flux equations, (5.12) and (5.13), which shows that the variation of $\overline{w'q'_t}$ and $\overline{w'\theta'_l}$ with height within the boundary layer can be calculated given the following information:

- Initial values of $\overline{\theta_l}$ and $\overline{q_t}$ within the boundary layer.
- Initial values of cloud base and cloud top heights.
- The jumps of $\overline{\theta_l}$ and $\overline{q_t}$ across the inversion.
- $F(z)$ specified through the cloud layer.
- That some measure of the entrainment rate w_e is available or that some relationship between w_e and other computed parameters exists.

If the model is to be used in a predictive capacity, the main problems arise in relating the entrainment process through w_e to the calculated turbulent characteristics and in determining whether the predicted structure is likely to remain well mixed. This requires, at minimum, some consideration of the turbulent kinetic energy balance within the boundary layer.

If the model is to be used to aid interpretation of observations it is still useful to diagnose quantities which are actually measured, i.e. $\overline{w'\theta'_v}$ or $\overline{w'q'_t}$.

5.2.1 The buoyancy flux in the stratocumulus-topped boundary layer

The mixed-layer model uses conserved variables. However, the vertical turbulent motions in an cloudy atmosphere are primarily driven by the buoyancy flux $(g/\overline{\theta_v})\overline{w'\theta'_v}$, so it is tempting to derive an expression that relates the fluxes of conserved variables $\overline{w'\theta'_l}$ and $\overline{w'q'_t}$ to the buoyancy flux (or the virtual potential temperature flux $\overline{w'\theta'_v}$). The virtual potential temperature flux in a saturated environment is given by,

$$\overline{w'\theta'_v} = \overline{w'\theta'}(1 + \epsilon_I \overline{q_s} - \overline{q_l}) + \overline{\theta}(\epsilon_I \overline{w'q'_s} - \overline{w'q'_l}), \tag{5.15}$$

where according to Eq. (2.12)

$$\epsilon_I = 1/\epsilon - 1 = R_v/R_d - 1 = 0.61, \tag{5.16}$$

and $\overline{w'q'_s}$ represents the saturated water vapor flux. In the unsaturated subcloud layer all the water is in the vapor phase ($q_l = 0$ and $q_t = q_v$), so in that case the virtual temperature flux reduces to

$$\overline{w'\theta'_v} = \overline{w'\theta'}(1 + \epsilon_I \overline{q_t}) + \overline{\theta}\epsilon_I \overline{w'q'_t}. \tag{5.17}$$

For unsaturated conditions we also have that the liquid water potential temperature flux reduces to the potential temperature flux $\overline{w'\theta'_l} = \overline{w'\theta'} - (L_v/c_p)\overline{w'q'_l} = \overline{w'\theta'}$. Thus, for an unsaturated atmosphere the virtual potential temperature flux in terms of conserved variables reads

$$\overline{w'\theta'_v} = \overline{w'\theta'_l}(1 + \epsilon_I \overline{q_v}) + \overline{\theta}\epsilon_I \overline{w'q'_t} = A_d \overline{w'\theta'_l} + B_d \overline{w'q'_t}, \tag{5.18}$$

by which we have defined the coefficient $A_d \approx 1.01$ and $B_d \approx 170$ for dry convection.

For the cloud layer the derivation is less straightforward. With aid of Eq. (5.16) and using that $q_t = q_s + q_l$ we can write

$$\epsilon_I q_s - q_l = (1 + \epsilon_I)q_s - q_t = \frac{q_s}{\epsilon} - q_t. \tag{5.19}$$

Using this expression we can rewrite Eq. (5.15):

$$\overline{w'\theta'_v} = \overline{w'\theta'}(1 + \frac{\overline{q_s}}{\epsilon} - \overline{q_t}) + \overline{\theta}(\frac{\overline{w'q'_s}}{\epsilon} - \overline{w'q'_t}). \tag{5.20}$$

The Clausius-Clapeyron equation (1.55) can be expressed in terms of the saturation specific humidity,

$$\frac{dq_s}{dT} = \frac{q_s l_v}{R_v T^2}. \tag{5.21}$$

If we write $dq_s = q'_s$ and $dT = T'$ then saturation specific humidity fluctuations are uniquely related to perturbations in the temperature,

$$q'_s = \frac{q_s l_v}{R_v T^2} T' \qquad \Longleftrightarrow \qquad q'_s = \left(\frac{dq_s}{dT}\right) T'. \tag{5.22}$$

This facilitates to write the saturation specific humidity flux as a (potential) temperature flux,

$$\overline{w'q'_s} = \left(\frac{dq_s}{dT}\right) \overline{w'T'} \approx \left(\frac{dq_s}{dT}\right) \overline{w'\theta'}, \tag{5.23}$$

where the error in the last approximation is less then a few percent. No we can substitute $\overline{w'q'_s}$ out of (5.20) to obtain

$$\overline{w'\theta'_v} = \overline{w'\theta'} \left[1 + \frac{\overline{q_s}}{\epsilon} - \overline{q_t} + \frac{\overline{\theta}}{\epsilon}\left(\frac{dq_s}{dT}\right)\right] - \overline{\theta}\overline{w'q'_t}. \tag{5.24}$$

Next, we use $\overline{w'\theta'} = \overline{w'\theta'_l} + (L_v/c_p)\overline{w'q'_l}$ to give

$$\begin{aligned} \overline{w'\theta'_v} = {} & \overline{w'\theta'_l} \left[1 + \frac{\overline{q_s}}{\epsilon} - \overline{q_t} + \frac{\overline{\theta}}{\epsilon}\left(\frac{dq_s}{dT}\right)\right] \\ & + \overline{w'q'_l}\left(\frac{L_v}{c_p}\right)\left[1 + \frac{\overline{q_s}}{\epsilon} - \overline{q_t} + \frac{\overline{\theta}}{\epsilon}\left(\frac{dq_s}{dT}\right)\right] - \overline{\theta}\overline{w'q'_t}. \end{aligned} \tag{5.25}$$

Last, we would like to substitute out the liquid water flux $\overline{w'q'_l}$. To this end we write

$$\begin{aligned} \overline{w'q'_l} &= \overline{w'q'_t} - \overline{w'q'_s} = \overline{w'q'_t} - \left(\frac{dq_s}{dT}\right)\overline{w'\theta'} \\ &= \overline{w'q'_t} - \left(\frac{dq_s}{dT}\right)\left[\overline{w'\theta'_l} + \left(\frac{L_v}{c_p}\right)\overline{w'q'_l}\right], \end{aligned} \tag{5.26}$$

which yields for $\overline{w'q'_l}$

$$\overline{w'q'_l} = \frac{\overline{w'q'_t}}{1 + \frac{L_v}{c_p}\left(\frac{dq_s}{dT}\right)} - \frac{\overline{w'\theta'_l}\left(\frac{dq_s}{dT}\right)}{1 + \frac{L_v}{c_p}\left(\frac{dq_s}{dT}\right)}. \tag{5.27}$$

The final expression for the virtual potential temperature flux in a saturated atmosphere is then given by

$$\overline{w'\theta_v'} = A_w \overline{w'\theta_l'} + B_w \overline{w'q_t'}, \tag{5.28}$$

with coefficients A_w and B_w having a weak temperature dependency,

$$A_w = \frac{1 + \frac{\overline{q_s}}{\epsilon} - \overline{q_t} + \frac{\overline{\theta}}{\epsilon}\left(\frac{dq_s}{dT}\right)}{1 + \frac{L_v}{c_p}\left(\frac{dq_s}{dT}\right)} \approx 0.5, \tag{5.29}$$

and

$$B_w = A_w \left(\frac{L_v}{c_p}\right) - \overline{\theta} \approx 1100. \tag{5.30}$$

In summary, from Eqs. (5.12) and (5.13) we can obtain the vertical fluxes for q_t and θ_l, respectively. Given these fluxes, the buoyancy fluxes in the subcloud and cloud layer follow straightforwardly from Eqs. (5.18) and (5.28), respectively.

With the mixed-layer model we are capable to address the following questions:

• How does the buoyancy flux profile in the stratocumulus-topped boundary layer look like?

• Turbulent eddies are capable to penetrate into the inversion layer and mix free atmosphere air into the boundary layer. One may intuitively argue that more buoyancy production of turbulent kinetic energy will support more entrainment. Is this indeed the case?

• What is cloud-top entrainment instability?

• Sometimes a two-layer turbulence structure is found in the stratocumulus-topped boundary layer. During the day this is often due to cloud warming by the absorption of shortwave radiation which can lead to a local stable stratification near the cloud base. How can we explain a decoupling between the subcloud and cloud layer during the night?

5.3 Results from a mixed-layer model

We computed flux profiles for nocturnal stratocumulus with the mixed-layer model for different entrainment rates. The boundary conditions are displayed in Table 5.1. During the night there is no solar radiation, and the longwave radiation profile is based on Figure 4.5, with $F_3 = 70$ W/m^2 and linearly decreasing to a zero net radiative flux over a downward vertical distance of 30 m ($F = 0$ W/m^2 for $z < z_i - 30$m).

Figure 5.2 shows that the total water flux is linear with height. For all entrainment rates shown, the flux gradient is positive indicating that for the examples

Parameter	value	units
$\overline{w'\theta'_{l0}}$	0.0033	mKs^{-1}
$\overline{w'q'_{t0}}$	0.007	ms^{-1}(g kg^{-1})
$\Delta\overline{\theta_l}$	6.2	K
$\Delta\overline{q_t}$	-1.2	g kg^{-1}
cloud base	240	m
cloud top	755	m

Table 5.1: Boundary conditions used for the mixed-layer model.

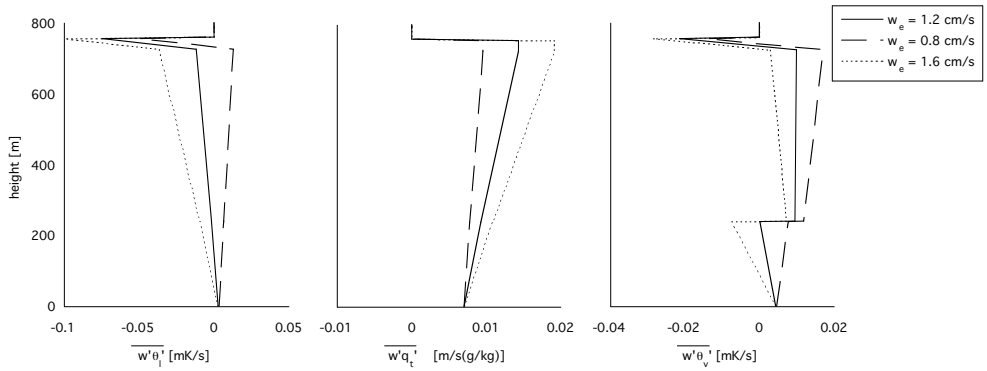

Figure 5.2: Vertical flux profiles computed with a mixed-layer model. Shown are $\overline{w'\theta'_l}$ (left panel), $\overline{w'q'_t}$ (middle panel) and $\overline{w'\theta'_v}$ (right panel). The three lines indicate results obtained for different entrainment rates, 0.8 (dashed line), 1.2 (solid line) and 1.6 (dotted line) cms^{-1}, respectively.

shown entrainment drying exceeds the turbulent flux of moisture from the surface. The case with the largest entrainment rate has the largest drying rate of the boundary layer. The liquid water potential temperature flux has a sharp jump at the boundary-layer top due the longwave radiative flux divergence; below this radiatively cooled layer the flux is linear with height.

Most particular is the shape of the virtual potential temperature flux profile. Because the fluxes of q_t and θ_l are continuous near the cloud base the jump of $\overline{w'\theta'_v}$ must be due to the different coefficients used in Eqs. (5.18) and (5.28). Because $A_w < A_d$ and $B_w > B_d$, the positive values for $\overline{w'\theta'_v}$ are predominantly due to latent heat release effects incorporated in the total water flux. Although at the top of the boundary layer $\overline{w'\theta'_v} < 0$ by entrainment of warm air, the entrainment warming is more than compensated by the longwave radiative cooling as just below the radiatively cooled layer the virtual potential temperature flux is positive.

It is interesting to note that smaller values for $\overline{w'\theta'_v}$ are associated with larger entrainment rates. The interpretation is that more entrainment leads to more downward mixing ($w' < 0$) of warm air ($\theta'_v > 0$) which tends to diminish the buoyancy flux.

Last, a careful inspection of magnitude of the virtual potential temperature flux below the cloud base shows that it can become negative. This implies that at the top of the subcloud layer the upward motions of the relatively moist thermals driven from the surface are damped. If the virtual potential temperature flux is sufficiently negative, the thermals may not be capable anymore to penetrate into the cloud layer. In that case the transport from moisture from the surface into the cloud layer is significantly reduced or even cut off, a situation which is referred to as decoupling. Because entrainment continues to mix in warm and dry air from above, decoupling can lead to a rapid thinning of the cloud layer.

5.3.1 Buoyancy reversal

The virtual potential temperature flux at the top of the cloud layer can be written as

$$\overline{w'\theta'_{vT}} = A_w\overline{w'\theta'_{lT}} + B_w\overline{w'q'_{tT}} = -w_e(A_w\Delta\overline{\theta_l} + B_w\Delta\overline{q_t}), \tag{5.31}$$

where we used the entrainment-jump relation (5.5). If

$$\Delta\overline{\theta_l} < -\frac{B_w}{A_w}\Delta\overline{q_t} \tag{5.32}$$

the virtual potential temperature flux due to entrainment becomes positive, $\overline{w'\theta'_{vT}} > 0$. For $\Delta\overline{q_t}$ in g/kg, $B_w/A_w \approx 2.2$. The physical interpretation of this finding is as follows. If warm and dry air from above the inversion is entrained and subsequently mixed into the cloud layer, the mixed parcel will experience some cooling

due to the evaporation of cloud droplets. Under certain conditions, the cooling will more than compensate the warming due to entrainment, and as a result the mixed parcel will become negatively buoyant with respect to its environment, which is referred to as *buoyancy reversal*. Because a negatively buoyant parcel will have a higher density with respect to its environment, it will sink and generate turbulent kinetic energy, promoting further entrainment. This process is called *cloud-top entrainment instability* (CTEI). It has been suggested that CTEI can lead to a rapid dissipation of stratocumulus, or, that it might be important in the transition from stratocumulus to cumulus (Randall, 1980; Deardorff, 1980).

Several CTEI criteria have been proposed in the literature based on different physical assumptions or from a laboratory study. Nevertheless, none of the proposed CTEI criteria has been generally accepted as being a mechanism responsible for stratocumulus break-up. On the contrary, Kuo and Schubert (1988) analyzed rawinsonde soundings presented in the literature to evaluate the CTEI criterion (5.32), and the effects of CTEI on cloud amount, and concluded that stratocumulus can persist for extended periods, even though the CTEI criterion was satisfied.

5.4 Entrainment

From the analysis with the mixed-layer model it is clear that the entrainment fluxes of heat and moisture play a major role in determining the evolution of the cloud layer. From this perspective it is rather unfortunate that there are only a few measurements available of the entrainment rate in stratocumulus clouds. There are a few different approaches possible to estimate the entrainment rate from observations.

First, we could use observations of the temporal evolution of the cloud-top height (z_i) from remote-sensing devices or tethered-balloon observations, and utilize Eq. (5.6), which is repeated here for convenience,

$$\frac{dz_i}{dt} = w_e + \overline{w}.$$

As an example, Figure 5.3 displays the inversion height which approximately corresponds to the cloud-top height. If one would have information of the subsidence rate Eq. (eq:zi) would then straightforwardly give the entrainment rate. The difficulty of this approach is that the large-scale subsidence $\overline{w}$ at cloud top is on the order of 1 cms^{-1} and hard to measure, although some researchers have used the horizontal wind velocities from observations like radiosondes to estimate $\overline{w}$ from the continuity equation ($\partial\overline{w}/\partial z = -(\partial\overline{u}/\partial x + \partial\overline{v}/\partial y)$. Otherwise, estimations for

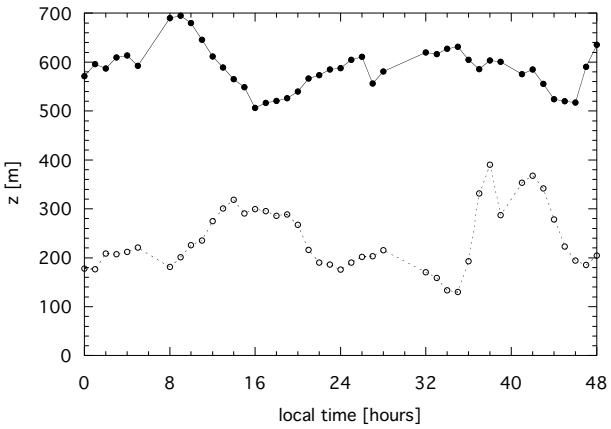

Figure 5.3: The cloud-base (open circles connected by the dashed line) and cloud-top height (filled circles and solid line) from observations as a function of time for 14 and 15 July 1987 (denoted from 0 to 48 hours Local Time). The plot symbols are according to the legend. Cloud-base height was measured by a Väisälä CT 12K laser ceilometer and a sodar was used to estimate the inversion height capping the cloud top. These instruments were operated on San Nicolas island, approximately $33°15'N$ and $119°30'W$, to monitor cloud properties with a high temporal resolution. The cloud layer depth shows a distinct diurnal cycle. During the night the cloud layer becomes thicker, but during the day there is a gradual thinning due to cloud warming by the aborption of solar radiation.

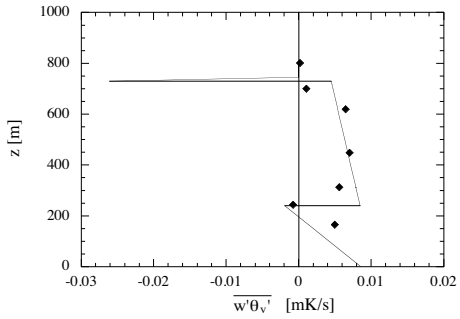

Figure 5.4: Aircraft observations of the virtual potential temperature flux (black diamonds) in a stratocumulus-topped boundary layer over the Atlantic Ocean during ASTEX. The mixed-layer model was utilized to estimate the entrainment rate by fitting the computed virtual potential temperature flux (solid line) to the observations. For this case an entrainment rate of 0.93 cms^{-1} was found. *From Duynkerke et al. (1995).*

$\overline{w}$ may be taken from General-Circulation Models, although the modeled large-scale vertical velocity fields do sometimes exhibit unphysical oscillations which casts some doubt on its accuracy. Also note that the inversion height may change by large-scale horizontal advection, provided the presence of a large-scale horizontal gradient in the inversion height.

Second, aircraft observations of turbulent fluxes of conserved variables at different heights can be used. If it is assumed that the boundary layer is in a quasi-steady state, the fluxes will be linear and the flux just below cloud top can be extrapolated from the observations. If the jump across the inversion is measured, the flux-jump relation ($w_e = -\overline{w'\psi'}_T/\Delta\overline{\psi}$) can be applied. The quantity ψ may be the total specific humidity, ozone, or dimethyl sulfide (DMS). In principle, with aid of Eq. (5.13) this approach can also be used for θ_l or θ_e, but this requires to take the radiative flux divergence into account.

Third, one can do a budget study by analysis of the variation with time for mean quantities in the boundary layer. In the absence of sources and sinks, the tendencies are controlled only by the surface and entrainment fluxes.

Last, given observations of the buoyancy flux, the mixed-layer model can be used as a diagnostic tool to estimate the entrainment rate. If measurements are available of the radiation profile and the boundary conditions similar to the quantities shown in Table 5.1 one can fit the mixed-layer model buoyancy flux profile to the observations. Figure 5.4 gives an example of this approach.

In the following we will explore whether similarity relationships for the clear

convective boundary layer (CBL) can be applied to stratocumulus. In the CBL the virtual potential temperature flux is linear with height (see Figure 4.7), and its value at the top of the mixed layer is approximately a constant fraction $A \approx 0.2$ of the surface flux,

$$\overline{w'\theta'_{vT}} = -w_e \Delta\overline{\theta_v} = -A\overline{w'\theta'_{v0}}, \tag{5.33}$$

where we used the flux-jump relation (5.5). The convective scaling velocity w_* gives a measure of the buoyancy flux production of turbulent kinetic energy and is defined as

$$w_* = \left[2.5\frac{g}{\theta_0}\int_0^{z_i} \overline{w'\theta'_v} dz\right]^{1/3}. \tag{5.34}$$

Note that for $A = 0.2$ the factor 2.5 in Eq. (5.34) cancels if one computes the integral with the flux at the top given by (5.33) :

$$w_*^3 = 2.5\frac{g}{\theta_0}\int_0^{z_i}\left[\overline{w'\theta'_{v0}}(1-\frac{z}{z_i}) + \overline{w'\theta'_{vT}}\frac{z}{z_i}\right] dz = \frac{g}{\theta_0}\overline{w'\theta'_{v0}} z_i. \tag{5.35}$$

By defining a Richardson number Ri_{w_*} for convectively driven layers,

$$Ri_{w_*} = \frac{g z_i}{\theta_0}\frac{\Delta\overline{\theta_v}}{w_*^2}, \tag{5.36}$$

we can express a scaling relation for the entrainment rate

$$\frac{w_e}{w_*} = A Ri_{w_*}^{-1}. \tag{5.37}$$

This formula predicts the entrainment rate in the CBL, and it is interesting to see whether it may also be applied to stratocumulus. Entrainment rates have been determined on the basis of observations made by aircraft in stratocumulus over the North Sea and the Atlantic Ocean. The latter case was part of ASTEX (Atlantic Stratocumulus to Cumulus Transition Experiment), a large field experiment dedicated to the study the transition of stratocumulus to cumulus in the Hadley circulation. Figure 5.5 shows systematic larger values for the entrainment rate in stratocumulus which suggests that the entrainment rate is larger than in the CBL.

Entrainment rate parametrizations often include the convective velocity scale w_* as measure of the buoyancy forcing. Scaling the entrainment rate in stratocumulus is complicated not only because the buoyancy flux depends on the entrainment rate, but also since the number of free parameters that determine the vertical profile of the buoyancy flux is much larger than that for the dry convective boundary layer. In the latter case, the entrainment rate is proportional to

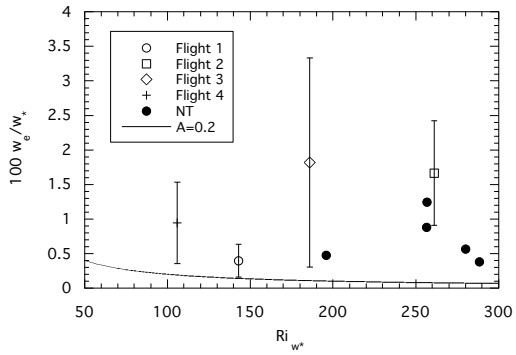

Figure 5.5: Flux-derived entrainment rates with error bars as a function of the convective Richardson number Ri_{w_*} for Flights 1-4 from the ASTEX First Lagrangian. Also plotted are aircraft-derived entrainment rates by Nicholls and Turton (1986) ('NT') and the scaling relation for the entrainment in the clear convective boundary layer, Eq. (5.37) with $A = 0.2$. Symbols and lines are according to the legend. *From De Roode and Duynkerke (1997).*

the ratio of the surface buoyancy flux $\overline{w'\theta'_v}_0$ and the buoyancy jump across the inversion $\Delta\theta_v$. However, according to Eq. (5.28) the total water flux gives a large contribution to the buoyancy flux in a stratocumulus cloud layer, which is due to the condensation and evaporation of liquid water droplets. For this reason, the surface moisture flux, the total specific humidity jump across the inversion, the cloud-base and cloud-top heights, and the long-wave radiative flux divergence at the cloud top (ΔF_l) are all relevant quantities. In summary, if we assume that the entrainment rate depends on the vertical profile of the buoyancy flux, a general scaling expression will depend on the following quantities

$$w_e = f(\overline{w'\theta'_v}(z)) = f(\overline{w'\theta'_l}_0, \overline{w'q'}_0, \Delta\theta_l, \Delta q_t, c_b, c_t, \Delta F_l). \tag{5.38}$$

In addition, short-wave radiative absorption in the cloud layer during daytime, windshear, and drizzle also affect the buoyancy flux profile. The sensitivity of the buoyancy flux to the quantities summarized above, and the role of the entrainment rate on the buoyancy flux vertical profile can all be clearly illustrated by means of a mixed layer model.

Chapter 6

Shallow Cumulus Clouds

6.1 Introduction

Figure 6.1 shows a detailed satellite image of shallow cumuli over Florida. An important feature of a cumulus cloud layer is that the mean relative humidity is below saturation, $RH < 100\%$. The typical cumulus cloud cover can be rather low, on the order of 0.1. Their vertical extent is about $1 \sim 2$ km, which is small enough to be non-precipitative. If the cumuli get deeper, precipitation becomes increasingly important and will interact with the dynamics. Despite their low cloud cover, shallow cumuli play an important role in transporting heat, moisture and pollutants from the boundary layer to the free atmosphere. As a simple, yet illustrative example of cumulus convection we will limit ourselves to shallow cumulus clouds, which are, by the absence of precipitation, also referred to as fair-weather cumulus.

As a first step to understanding the presence of cumulus clouds we will study air parcels that rise isentropically. Second, we will use observations as a basis for explaining some generic features of shallow cumuli. The Chapter 'Shallow cumulus convection' written by Pier Siebesma (1998) in the book 'Buoyant Convection in Geophysical Flows' covers more topics than this Chapter.

6.2 Thermodynamics

6.2.1 Stability and temperature lapse rates

6.2.2 Atmospheric stability

The thermodynamic stability of the atmosphere is important in the description of the structure of the cumulus-topped boundary layer. The stability is usually

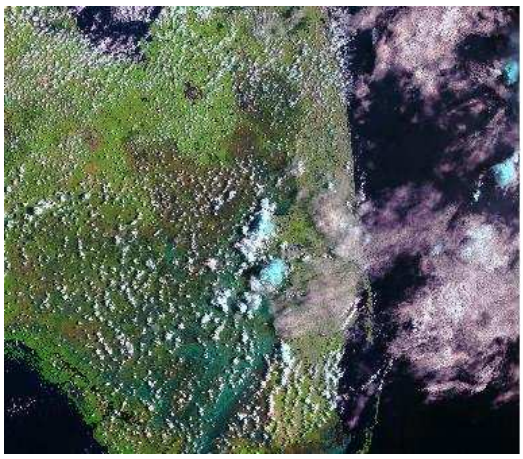

Figure 6.1: Shallow cumulus over Florida. *Courtesy of Stephaan Rodts.*

defined by the sign of the buoyant force on a vertically displaced air parcel. Consider a parcel of air with a virtual temperature $T_{v,p}$ in an environment with average properties $\overline{T_v}(z)$. In the Boussinesq approximation, the net buoyant force F_B per unit mass acting on the parcel is given by Rogers and Yau (1989),

$$F_B = g\frac{T_{v,p} - \overline{T_v}}{T_0}. \tag{6.1}$$

In this equation it is assumed that the parcel's pressure adjusts instantaneously to the environmental pressure ($p_p = \overline{p}$). If we displace the parcel from a height z over an infinitesimal distance δz and if the buoyancy is the only force acting on the parcel, then the vertical velocity is given by Newton's second law of motion,

$$\frac{dw}{dt} = \frac{d^2\delta z}{dt^2} = F_B(z + \delta z) - F_B(z) = \frac{dF_b}{dz}\delta z. \tag{6.2}$$

From Eq. (6.2) we recognize the equation of the harmonic oscillator whose solution is either oscillating or exponentially growing, depending on the sign of dF_B/dz,

$$\frac{d^2\delta z}{dt^2} = \frac{g}{T_0}\left(\frac{\partial T_{v,p}}{\partial z} - \frac{\partial \overline{T_v}}{\partial z}\right)\delta z \tag{6.3}$$

Therefore for any parcel the mean state is stable if

$$\frac{\partial T_{v,p}}{\partial z} < \frac{\partial \overline{T_v}}{\partial z} \qquad \Longleftrightarrow \qquad \textit{stable} \tag{6.4}$$

The vertical lapse rate of the mean virtual potential temperature determines whether cumuli may develop. We have already seen that the dry-adiabatic lapse rate is given by

$$\Gamma_d \equiv -\left(\frac{dT}{dz}\right) = \frac{g}{c_p}, \tag{6.5}$$

and we would like to derive a analogous expression for the wet-adiabatic lapse rate. To this end we will consider an isentropically rising air parcel that does not mix with its environment. The most convenient quantities to use are the liquid water potential temperature and the total water content which will be conserved for the process:

$$\theta_l = \theta - \frac{l_v}{c_p} q_l = constant \qquad , \qquad q_t = q_s + q_l = constant. \tag{6.6}$$

Here we will neglect the influence of moisture on the specific heat capacity $c_{pm} \approx c_p$, and we use the linearized form of the liquid water potential temperature. Because θ_l and q_t are constant we can also write for the parcel:

$$\frac{d\theta}{dz} + \frac{l_v}{c_p}\frac{dq_s}{dz} = 0. \tag{6.7}$$

This will be our starting point in deriving the wet-adiabatic lapse rate. The attentive reader will have noticed that the equation above is equivalent to stating that the equivalent potential temperature of the parcel is constant with height:

$$\frac{d\theta_e}{dz} \equiv \frac{d\theta}{dz} + \frac{l_v}{c_p}\frac{dq_*}{dz} = 0. \tag{6.8}$$

where $q_* = q_t$ if $q_t < q_s$, and $q_* = q_s$ for saturation, $q_t > q_s$.

To compute the vertical gradient of the saturation specific humidity we will use the Clausius-Clapeyron equation, repeated here for convenience,

$$\frac{\partial e_s}{\partial T} = \frac{l_v e_s}{R_v T^2}. \tag{6.9}$$

The saturation specific humidity is given by

$$q_s = \frac{\epsilon e_s}{p + e_s(\epsilon - 1)}, \tag{6.10}$$

with $\epsilon = R_d/R_v$. Because q_s depends on the partial water vapor saturation pressure e_s and the mean pressure p we have

$$dq_s = \frac{dq_s}{de_s}de_s + \frac{dq_s}{dp}dp = \frac{dq_s}{de_s}\frac{de_s}{dT}dT + \frac{dq_s}{dp}dp. \tag{6.11}$$

Differentiating Eq. (6.10) with respect to e_s and p yields, respectively,

$$\frac{dq_s}{de_s} = \frac{\epsilon p}{[p + e_s(\epsilon - 1)]^2}, \tag{6.12}$$

$$\frac{dq_s}{dp} = -\frac{e_s \epsilon}{[p + e_s(\epsilon - 1)]^2}. \tag{6.13}$$

Substituting these two expressions, and Eq. (6.9) into Eq. (6.11) gives

$$dq_s = \frac{q_s}{p + e_s(\epsilon - 1)} \left(\frac{p l_v}{R_v T^2} dT - dp \right). \tag{6.14}$$

If we rewrite Eq. (6.10) as

$$e_s = \frac{q_s p}{\epsilon + q_s(1 - \epsilon)} \tag{6.15}$$

then we can substitute e_s out of Eq. (6.14),

$$dq_s = \left(1 + \frac{1 - \epsilon}{\epsilon} q_s \right) \left(\frac{q_s l_v}{R_v T^2} dT - q_s \frac{dp}{p} \right). \tag{6.16}$$

The potential temperature depends on the temperature and the pressure, thus

$$d\theta = \frac{d\theta}{dT} dT + \frac{d\theta}{dp} dp = \frac{\theta}{T} dT - \frac{R_d \theta}{c_p p} dp. \tag{6.17}$$

We have now expressed dq_s and $d\theta$ in terms of dT and dp. As we are interested in the vertical derivative of the temperature dT/dz we need to evaluate dp/dz. For this purpose we can use the gas law and if we assume that the atmosphere is in a hydrostatic equilibrium then it follows

$$\frac{dp}{dz} = -\rho g = -\frac{pg}{R_d T_v}. \tag{6.18}$$

We have now taken all the necessary steps to write the wet-adiabatic lapse rate as

$$\frac{dT}{dz} = -\left[\frac{\frac{\theta}{T}\frac{g}{c_p} + \frac{l_v}{c_p}(1 + \frac{1-\epsilon}{\epsilon} q_s)\frac{q_s g}{R_d T_v}}{\frac{\theta}{T} + \frac{l_v}{c_p}(1 + \frac{1-\epsilon}{\epsilon} q_s)\frac{q_s l_v}{R_v T^2}} \right]. \tag{6.19}$$

In the literature one often finds a simplified expression. In particular, if one approximates $\theta/T \approx 1$, $T_v \approx T$ and because in the atmosphere typically $q_s < 4 \cdot 10^{-2}$ kg·kg^{-1} the wet-adiabatic lapse rate Γ_m can be expressed as

$$\Gamma_m = -\frac{dT}{dz} = \Gamma_d \left[\frac{1 + \frac{q_s l_v}{R_d T}}{1 + \frac{l_v^2 q_s}{c_p R_v T^2}} \right] < \Gamma_d. \tag{6.20}$$

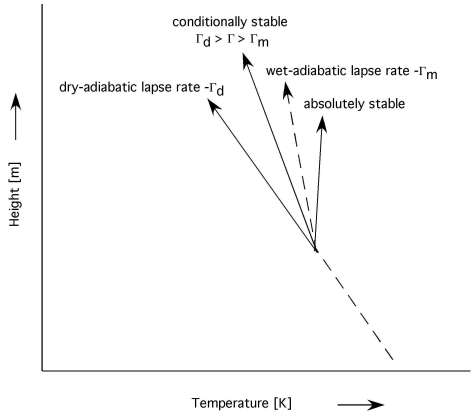

Figure 6.2: Lapse rates and stability. The dashed line indicates the temperature as a function of height for an isentropically rising air parcel.

The inequality is satisfied whenever $l_v\epsilon > c_pT$. Because of the high value of l_v for water, this inequality is always valid in the atmosphere. The release of latent heat in a saturated parcel explains why the moist adiabatic lapse rate Γ_m is always smaller than the dry adiabatic lapse rate Γ_d. Its actual value depends strongly on the temperature, and to a lesser extent on the mean pressure. For $T = 288$ K and $p = 1000$ hPa we find $\Gamma_m = 4.3$ K/km. For lower temperatures however the difference between Γ_m and Γ_d becomes progressively smaller.

The virtual temperature lapse rate of an isentropically rising parcel can be computed along the same lines as the temperature lapse rate. If we for simplicity ignore the effect of water vapor and liquid water on the vertical gradient of the virtual temperature we can define the following stability criteria:

$$\begin{aligned} (-\partial\overline{T}/\partial z) > \Gamma_d \quad &\Longleftrightarrow \quad \textit{Absolute instability} \\ \Gamma_m < (-\partial\overline{T}/\partial z) < \Gamma_d \quad &\Longleftrightarrow \quad \textit{Conditional instability} \\ (-\partial\overline{T}/\partial z) < \Gamma_m \quad &\Longleftrightarrow \quad \textit{Absolute stability.} \end{aligned}$$

Absolute instability if often found near the surface when solar radiation is heating the ground surface, or if cold air is advected over relatively warm surfaces. If rising thermals penetrate a conditionally unstable layer they will be damped unless there is sufficient moisture in the thermals such that saturation can occur. In the latter case latent heat release effects will cause the thermal to remain warmer than its surrounding environment. Any convection, either dry or wet, will be damped if the temperature lapse rate of the atmosphere is absolutely stable. *For the development of active cumuli it is therefore necessary that the atmosphere is conditionally unstable.*

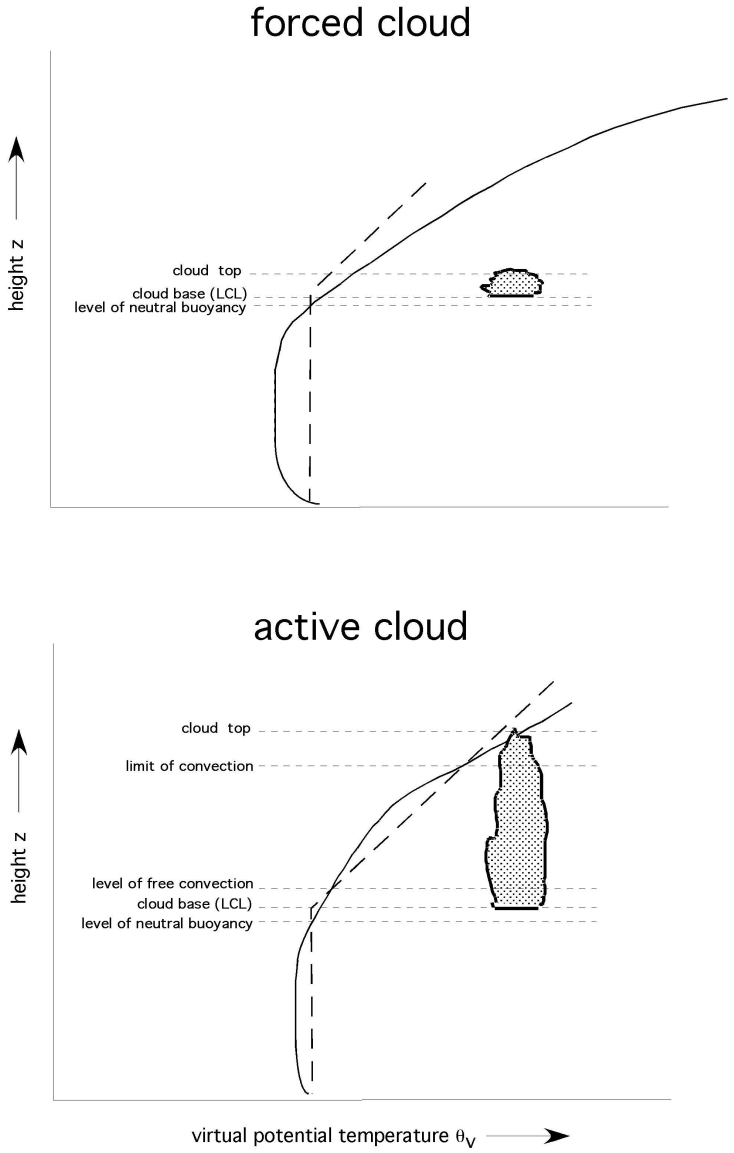

Figure 6.3: Schematic representation of key levels in shallow cumulus clouds which are related to condensation and buoyancy. The dashed lines represent the virtual potential temperature for an isentropically rising air parcel. In the subcloud layer it follows the dry adiaabatic lapse rate, but above the cloud base its virtual potential temperature increases with height according to the wet-adiabat due to the release of latent heat.

A schematic description of some important definitions in cumulus classification is given in Figure 6.3. Consider the full line as the virtual potential temperature of the environment. From the gradient at the surface it is obvious that the boundary layer is unstable. Suppose a thermal is induced by a small disturbance. When it isentropically rises it is cooled following the dry adiabatic lapse rate indicated by the vertical broken line. At the *level of neutral buoyancy* (LNB) the virtual temperature of the thermal equals the virtual potential temperature of the environment. Because the thermal has obtained a vertical velocity (inertia) it can penetrate slightly into the stable layer where it is gradually decelerated. When the thermal becomes saturated cloud droplets are formed. This level defines the cloud base and is also denoted as the *lifting cloud condensation level* (LCL). Because of latent heat release the cloud parcel will follow the wet-adiabatic lapse rate above the LCL.

From this stage there are two possible scenarios. If the lapse rate of the environment is larger than the wet-adiabatic lapse rate, the cloud parcel will remain negatively buoyant with respect to its environment. As a result its vertical motion will be damped and its vertical growth will be limited. Such a cloud is called a *forced* cloud. In contrast, when the lapse rate of the virtual potential temperature of the environment is less than the wet-adiabatic lapse rate, the cloud may reach the *level of free convection* (LFC). At this level the cloud is exactly neutrally buoyant with respect to its environment, but above it can gain vertical momentum again by a positive buoyancy excess until it reaches the *limit of convection* (LOC). Due to the kinetic energy the cloud has obtained it can overshoot such that the actual cloud top is often observed above the LOC. This specific cloud type is able to vent air into the free atmosphere. For a cumulus cloud obeying this pattern the term *active* cloud is used.

It must be mentioned that this explanation is highly idealized. In reality the properties of a thermal will not be conserved as shown in Figure 6.3. By lateral mixing with environmental air the broken line will merely tend to bend towards the curve representing the environmental virtual potential temperature.

6.3 Observations

Although cumulus clouds are frequently occuring, our knowledge of these clouds is rather limited due to the relatively few aircraft measurements made. One of the earliest series of measurements in cumulus-cloud layers was presented by Warner (1955). He showed from aircraft penetrations through cumulus clouds that the liquid water content is substantially lower than its adiabatic value computed from an isentropically rising air parcel. Moreover, it was found that the ratio of the

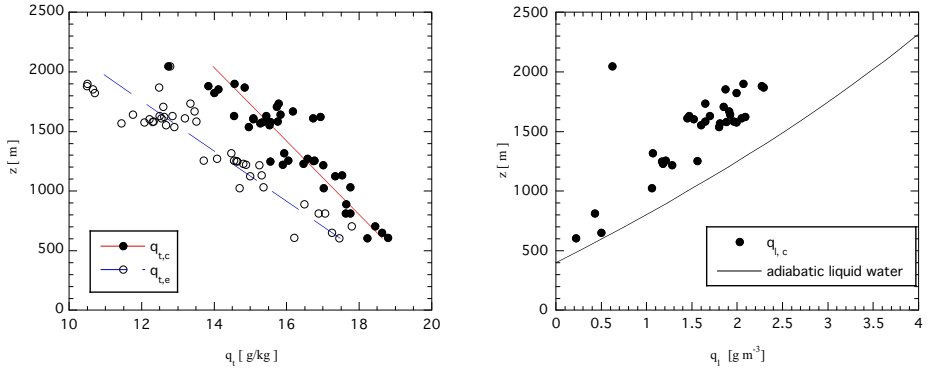

Figure 6.4: Example of conditionally sampled total water content values in shallow cumuli ($q_{t,c}$ and their environment (left panel), and the observed in-cloud liquid water content compared to the adiabatic lapse rate. The solid and dashed lines indicate linear fits. The observations were collected during SCMS.

measured liquid water content to its adiabatic value decreases systematically with height. This classic result has been confirmed by other authors, at least qualitatively, and is an indication that clouds continuously dilute by turbulent mixing with their environment.

A recent field experiment during which cumuli were observed took place in Cocoa Beech, Florida from 17 July-13 August 1995 as part of the Small Cumulus Microphysics Study (SCMS).The aircraft data were carefully analyzed by Rodts et al. (2003). Figure 6.4 shows an example of in-cloud total water content values and the cloud liquid water content from aircraft observations in a cumulus field over Florida during SCMS. The environmental total water content values gradually decrease with height as do the in-cloud values. The facts that the in-cloud total water content is not constant with height and that the cloud liquid water content is below the adiabatic value are in line with findings from other experiments and implies that clouds mix air with their environment. This process is usually referred to as *lateral entrainment*, and indicates that matters are much more complicated than the idealized situation in which we considered a rising parcel that does not mix with its environment. Because the lateral mixing tends to decrease the buoyancy excess of the cloud, it directly affects the vertical velocity and the cloud top height. It is therefore crucial to understand the dynamics and mixing mechanisms of cumulus clouds with their environment.

Figure 6.5 nicely illustrates the intermittent character of cumulus convection Over a horizontal distance of about 100 km there only are five cloud spots in which the vertical velocity field exhibits large fluctuations indicating a high level

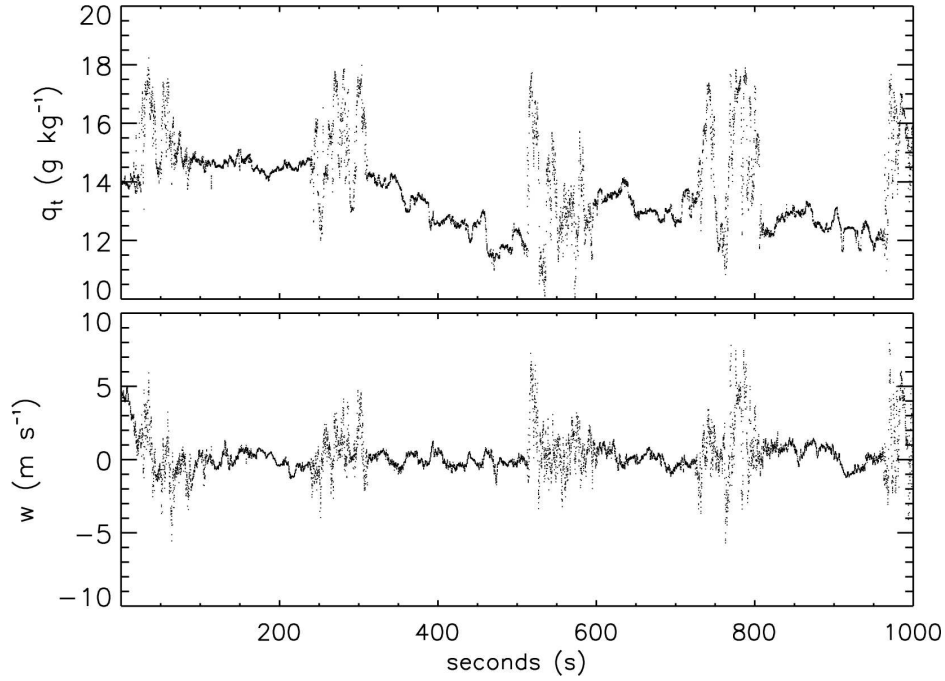

Figure 6.5: Example of a time series measured in a cumulus field during the SCMS experiment which took place over Florida, August 5, 1995: (top) total water content; (bottom) vertical velocity. The aircraft speed was about 100 ms^{-1}, and therefore the length of the data series is about 100 km. *From Rodts (2001).*

of turbulence inside and in the near vicinity of the clouds. Farther away from the clouds the atmosphere is nearly laminar. Notice the large upward vertical velocities in the cloud ($w > 5\text{ms}^{-1}$) and the presence of strong *downdrafts*.

To obtain averaged cumulus cross-section profiles four aircraft were used and all clouds larger than 500 m were rescaled to unit length. All in-cloud measurement points of an observed quantity were divided into 10 equidistant bins. In order to compare the cumulus cross section with its environment the same procedure was followed for the out-cloud regions: an equal amount of out-cloud measurement points was taken before the aircraft flew into a cloud and after the aircraft exited the cloud. Also these observations were rescaled to unit length and divided into 10 equidistant bins. The results are plotted on a scale ranging from -1 to 2, where the interval $[0, 1]$ pertains the cloudy region. Evidently, since the airplane penetrated clouds randomly, the results should be symmetric around 0.5, provided there are enough data points.

The results for the vertical velocity, the virtual potential temperature, the liquid water potential temperature and the total water content of the four flights are shown on the left of Figure 6.6. All profiles have a quite similar shape, although the absolute values differ from flight to flight. This is due to the fact that the boundary layer is slightly different each day. The in-cloud vertical velocities clearly is positive and are driven by a positive virtual potential temperature excess of the clouds. As the clouds originate from moist thermals triggered from the ground, the clouds have a larger total water content than their environment. For $\theta_{l,c}$, see exercise 2.

On the right of Figure 6.6 the height effect is eliminated and the four flights are averaged to one profile: the average value of the region before the aircraft penetrated the cloud was subtracted from all the measured values before binning and avaraging. The bars in the figure indicate the root-mean-square deviations from the mean and are a measure for the turbulence; they thus do *not* indicate the error in the measurements. The deviations are much higher inside the cloud than outside the cloud, as clouds are more turbulent than the environment. The vertical velocity in the cloud is on average between 1 and 2 ms^{-1}. On average the cloudy air moves upward, but just outside the cloud boundary a thin shell of air moving downward is found. As possible explanations, the downward velocities may be due to evaporative cooling after mixing with dry environmental air or by a mechanical forcing constrained by the continuity equation for mass.

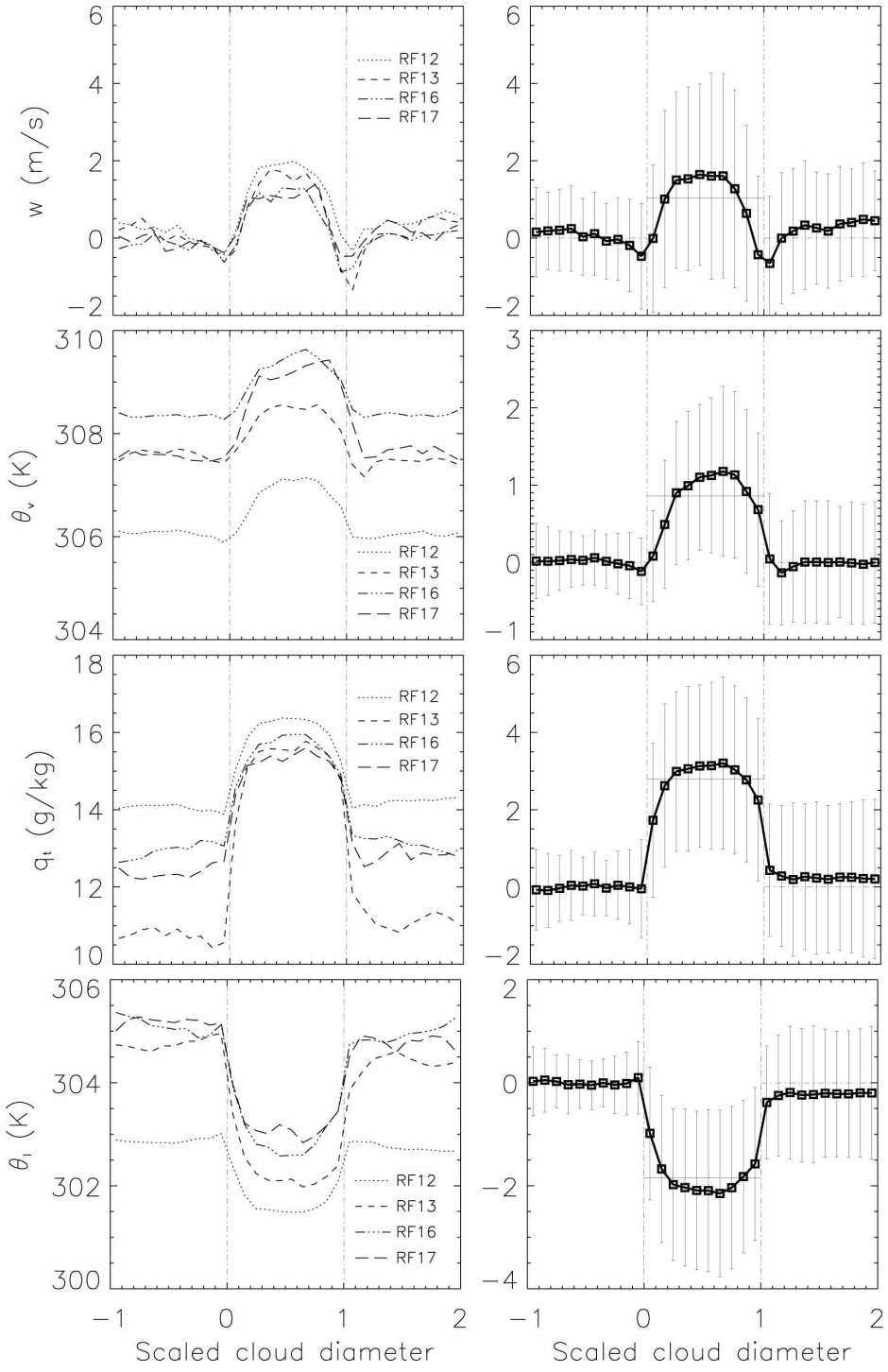

Figure 6.6: Averaged in-cloud profiles of the vertical velocity, virtual potential temperature, total water content and the liquid water potential temperature during four different research flights, labeled RF12, RF13, RF16 and RF17 (left). The plots on the right indicate average values of the four flights where the effect of altitude on the measurements is eliminated. The cloud is scaled between 0 and 1. The bars denote the root-mean-square values of the individual measurements. These bars thus do not denote an error.

6.4 Plume models

6.4.1 Conditional sampling technique

The conditionally sampled mean value $[\psi]_c$ is defined as

$$[\psi]_c = \frac{\int_A I_s \psi dA}{\int_A I_s dA}, \tag{6.21}$$

where the integration is performed over a horizontal plane at height z and I_s is an indicator function. $I_s = 1$ if a sampling criterion is met, and $I_s = 0$ otherwise. To determine properties of the cumulus clouds only, one usually samples on the presence of liquid water (q_l), although several other criteria are sometimes added. For instance, the cloud core is defined as the part of the cloud that has both an upward vertical velocity and a positive virtual potential temperature excess. A summary of sampling criteria that may be applied are summarized in Table 6.1.

Indicator function	Type	Sampling criteria
I_0	Slab mean	None
I_1	Updraft	$w > 0$
I_2	Cloud	$q_l > 0$
I_3	Cloud updraft	$q_l > 0$ and $w > 0$
I_4	Cloud downdraft	$q_l > 0$ and $w < 0$
I_5	Cloud core	$q_l > 0$ and $w > 0$ and $\theta_v > \overline{\theta_v}$

Table 6.1: Summary of sampling criteria. $\overline{\theta_v}$ is the horizontal mean value of the virtual potential temperature.

The sampled area fraction σ is defined as

$$\sigma = \frac{\int_A I_s dA}{\int_A dA}. \tag{6.22}$$

For a two-stream approximation (cloud/environment, updraft/downdraft, etcetera) we can define the fraction of the environment σ_e as

$$\sigma_e = 1 - \sigma. \tag{6.23}$$

By this definition the environment represents the area fraction of all points where the applied sampling criteria are not satisfied. In the remainder of this course the square brackets that indicate the conditionally sampled mean are, for notational convenience, replaced by the subscripts '$_c$' or '$_e$' except when the operator is

applied on a derivative. The horizontal slab-mean value is indicated by an overbar and is given by

$$\overline{\psi} = \sigma\psi_c + (1-\sigma)\psi_e. \tag{6.24}$$

The massflux M_c is defined as

$$M_c \equiv \rho\sigma(w_c - \overline{w}) = \rho\sigma(1-\sigma)(w_c - w_e). \tag{6.25}$$

but for notational convenience one sometimes uses a definition which does not involve the density,

$$M_c \equiv \sigma(w_c - \overline{w}) = \sigma(1-\sigma)(w_c - w_e). \tag{6.26}$$

where the 'massflux' has units ms^{-1}. In the remainder we will use the latter definition.

The continuity equation for mass is given by

$$\frac{\partial M_c}{\partial z} = -\frac{\partial \sigma}{\partial t} + E - D, \tag{6.27}$$

with E and D the lateral entrainment and detrainment rates, respectively. If $E > 0$, then air is entrained and subsequently mixed from the environment into the cloud, and vice versa for the detrainment $D > 0$.

If we conditionally sample the vertical flux we obtain

$$\begin{aligned}\overline{w'\psi'} &= \sigma[w'\psi']_c + (1-\sigma)[w'\psi']_e \\ &= \sigma(1-\sigma)(w_c - w_e)(\psi_c - \psi_e) + \sigma[w''\psi'']_c + (1-\sigma)[w''\psi'']_e,\end{aligned} \tag{6.28}$$

where the latter two terms indicate the so-called sub-plume fluxes, which are due to the contributions of perturbations with respect to the conditionally sampled mean. The 'top-hat' approach assumes that there are no fluctuations in the clouds or in their environment with respect to the conditionally sampled mean values, $\psi_c' = 0$ and $\psi_e' = 0$. In this approach, which is also called the 'massflux' approach, the fluctuations in the cloud, as measured by the bars in Figure 6.6, are taken to be zero. As a consequence of this assumption the sub-plume fluxes must vanish:

$$\sigma[w''\psi'']_c = (1-\sigma)[w''\psi'']_e = 0. \tag{6.29}$$

This is a core assumption in the description of (shallow) cumulus convection. A quick visual inspection of the time series for the vertical velocity and the total water content shows that this is a rather idealized assumption.

In case the subplume fluxes can be neglected, then the Reynolds-averaged flux can be simply expressed as

$$\overline{w'\psi'} = \sigma(1-\sigma)(w_c - w_e)(\psi_c - \psi_e) = M_c(\psi_c - \psi_e), \tag{6.30}$$

and the tendency of the mean $\overline{\psi}$ due to turbulent transport is then given by

$$\frac{\partial \overline{\psi}}{\partial t} = -\frac{\partial M_c(\psi_c - \psi_e)}{\partial z} + S_\psi. \tag{6.31}$$

In the massflux approach one can write separate equations for mean quantities in the cloud and its environment, respectively,

$$\frac{\partial \sigma \psi_c}{\partial t} = -\frac{\partial M_c \psi_c}{\partial z} + E\psi_e - D\psi_c + \sigma S_{\psi,c}, \tag{6.32}$$

$$\frac{\partial (1-\sigma) \psi_e}{\partial t} = +\frac{\partial M_c \psi_e}{\partial z} - E\psi_e + D\psi_c + (1-\sigma) S_{\psi,e}, \tag{6.33}$$

Lateral mixing

The results of the in-cloud total water content in Figure 6.4 indicate that as cumuli rise they mix air with their environment, meaning that the lateral entrainment rate $E \neq 0$. Because lateral mixing tends to decrease the buoyancy excess of the cloud it will therefore influence the vertical velocity of the cloud. Then the question arises how much air is mixed across the cloud boundaries?

To estimate the lateral entrainment rate we will make use of the mass flux equations, in particular the prognostic equation for ψ_c Eq. (6.32) and the continuity equation, Eq. (6.27). Let us assume that the cloud fraction does not change with time, then

$$\frac{\partial M_c}{\partial z} = +E - D, \tag{6.34}$$

Likewise, if we assume that the temporal change for ψ_c is small compared to the terms on the right-hand-side of Eq. (6.32), and if $S_{\psi,c} = 0$ we can write

$$-\frac{\partial M_c \psi_c}{\partial z} + E\psi_e - D\psi_c = 0. \tag{6.35}$$

With aid of Eq. (6.34) it is now straightforward to write and expression for ϵ,

$$\frac{E}{M_c} \equiv \epsilon = -\frac{\partial \psi_c / \partial z}{(\psi_c - \psi_e)} \tag{6.36}$$

by which we have defined the fractional, or normalized, entrainment ϵ rate. Likewise, the fractional detrainment rate $\delta \equiv D/M_c$.

Let us use the results displayed in Figure 6.4 to estimate the fractional entrainment rate. The linear fits for the in-cloud and environmental total water content, $q_{t,c}$ and $q_{t,e}$ in (g/kg) are, respectively,

$$\begin{aligned} q_{t,c}(z) &= 20.60 - 3.34z \\ q_{t,e}(z) &= 20.34 - 4.75z, \end{aligned} \tag{6.37}$$

with z in km. Given these expressions, we obtain $q_{t,c} - q_{t,e} = 1.76$ (g/kg) at $z = 1$ km, and consequently for this height $\epsilon = 1.9 \cdot 10^{-3}$ m^{-1}. This number is in agreement with other observational studies and detailed numerical simulations.

It is interesting to note that a previous version of the weather forecast model of the ECMWF the fractional entrainment rate for shallow cumuli was about a factor of 10 smaller than the number found in this example. In the model a too small fractional entrainment will lead to cumuli that are too active and rise too high. In the current version of the ECMWF model an more realistic value is used.

6.4.2 The vertical velocity equation

By a vertical integration of the cloud buoyancy between the level of free convection (z_{LFC}) and the limit of convection (z_{LOC}) the *convective available potential energy* (CAPE) of the atmosphere can be estimated:

$$CAPE = \frac{g}{\overline{\theta_v}} \int_{z_{LFC}}^{z_{LOC}} (\theta_{v,c} - \overline{\theta_v}) dz \tag{6.38}$$

A typical velocity scale, w_{CAPE} can be defined by assuming that all the potential energy is converted into kinetic energy. In the literature one finds the following definition:

$$w_{CAPE} = 2 \cdot (CAPE)^{1/2}. \tag{6.39}$$

The velocity scale is derived by neglecting pressure effects and assuming that there is no lateral mixing.

The conditionally sampled vertical velocity equation can be derived from by taking $\psi = w$ in Eq. (6.32) and treating the buoyancy and the pressure gradient terms as a source/sink contribution,

$$\frac{\partial \sigma w_c}{\partial t} = \frac{g}{\overline{\theta_v}} \sigma (\theta_{v,c} - \overline{\theta_v}) - \frac{\partial M_c w_c}{\partial z} - \sigma \left[\frac{\partial p}{\partial z} \right]_c + E w_e - D w_c. \tag{6.40}$$

For a steady-state solution, and if we neglect pressure effects and assume that there is no lateral mixing than the vertical velocity equation yields the following balance,

$$M_c w_c = \sigma \cdot CAPE \qquad \Longleftrightarrow \qquad w_c = (CAPE)^{1/2}, \tag{6.41}$$

where we neglected the subsidence term in the definition for the mass flux ($\overline{w} \ll w_c$). Obviously, this expression differs a factor of 2 from Eq. (6.39). How can we explain this? The difference arises from a different treatment of the advection term in the velocity equation. The definition for CAPE is based on the following equation,

$$\frac{\partial u_i}{\partial t} + u_j \frac{\partial u_i}{\partial x_j} = S_{u_i} \quad \Longleftrightarrow \quad (i = 3) \quad \frac{\partial w}{\partial t} + u \frac{\partial w}{\partial x} + v \frac{\partial w}{\partial y} + \frac{1}{2} \frac{\partial w w}{\partial z} = S_w. \tag{6.42}$$

By the continuity equation for mass, $\partial u_j/\partial x_j = 0$, we can write the advection term in flux form,

$$\frac{\partial u_i}{\partial t} + \frac{\partial u_i u_j}{\partial x_j} = S_{u_i} \quad \Longleftrightarrow \quad (i=3) \quad \frac{\partial w}{\partial t} + \frac{\partial uw}{\partial x} + \frac{\partial vw}{\partial y} + \frac{\partial ww}{\partial z} = S_w. \tag{6.43}$$

The conditionally sampled vertical velocity equation (6.40) is based on the latter equation. In fact, the factor of 2 is compensated by the horizontal flux divergence of the momentum transport term. In the sampled vertical velocity equation for $j \in \{1, 2\}$ the sampled horizontal advection term $u_j \partial w/\partial x_j$ and the momentum flux term, $\partial(u_j w)/\partial x_j$, are expressed as a lateral entrainment and detrainment term. Because one assumes a balance between buoyancy and the vertical velocity term, thereby neglecting lateral mixing, this explains the factor of 2 difference.

Exercises

1. Use Eq. (6.20) to compute the wet-adiabatic lapse rate as a function of temperature for the following pressures: 1000, 900 and 800 hPa.

2. Can you argue why the in-cloud liquid water content in Figure 6.6 is lower than its environment? *Hint*: Use the following definitions for the mean, $\overline{\theta_l} = \overline{\theta} - l_v/c_p\overline{q_l}$ and $\overline{\theta_v} = \overline{\theta}(1 + 0.61\overline{q_v} - \overline{q_l})$. Moreover, the cloud fraction is often on the order of $\sigma \approx 0.1$, so the mean liquid water content $\overline{q_l}$ of the cloud layer is relatively small compared to the in-cloud value. In that case, what can you say about $\overline{\theta_l}$ and $\overline{\theta_v}$? How will the in-cloud θ_l vertical profile look like if we assume that the cloud does not mix with its environment?

3. Show that $\rho\sigma(w_c - \overline{w}) = \rho\sigma(1-\sigma)(w_c - w_e)$. *Hint*: use the definition for the mean [Eq. (6.24)].

Bibliography

Bohren, C. F. and B. A. Albrecht, 1998: *Atmospheric Thermodynamics*. Oxford University Press, 402 pp.

De Roode, S. R. and P. G. Duynkerke, 1997: Observed Lagrangian transition of stratocumulus into cumulus during ASTEX: Mean state and turbulence structure. *J. Atmos. Sci.*, **54**, 2157–2173.

Deardorff, J. W., 1980: Cloud-top entrainment instability. *J. Atmos. Sci.*, **37**, 131–147.

Duynkerke, P. G., , H.-Q. Zhang, and P. J. Jonker, 1995: Microphysical and turbulent structure of nocturnal stratocumulus as observed during ASTEX. *J. Atmos. Sci.*, **52**, 2763–2777.

Duynkerke, P. G. and J. Teixeira, 2001: Comparison of the ECMWF reanalysis with FIRE I observations: Diurnal variation of marine stratocumulus. *J. Climate*, **14**, 1466–1478.

Garratt, J. R., 1994: *The atmospheric boundary layer*. Cambridge atmospheric and space science series, first paperback edition edition, 316 pp.

Gill, A. E., 1982: *Atmosphere-Ocean Dynamics*. Academic Press, New York, 662 pp.

Holton, J. R., 1992: *An Introduction to Dynamic Meteorology*. Academic Press, 511 pp.

Iribarne, J. V. and W. L. Godson, 1981: *Atmospheric Thermodynamics*. D. Reidel, 2nd ed. edition, 259 pp.

Kuo, H. and W. H. Schubert, 1988: Stability of cloud-topped boundary layers. *Q. J. R. Meteorol. Soc.*, **114**, 887–917.

Lorenz, E. N., 1955: Available potential energy and the maintenance of the general circulation. *Tellus*, **7**, 157–167.

Ma, C.-C., C. R. Mechoso, A. W. Robertson, and A. Arakawa, 1996: Peruvian stratus clouds and the tropical Pacific circulation: A coupled ocean-atmosphere GCM study. *J. Climate*, **9**, 1635–1645.

Nicholls, S., 1984: The dynamics of stratocumulus: Aircraft observations and comparisons with a mixed layer model. *Q. J. R. Meteorol. Soc.*, **110**, 783–820.

Nicholls, S. and J. D. Turton, 1986: An observational study of the structure of stratiform cloud sheets: Part II. Entrainment. *Q. J. R. Meteorol. Soc.*, **112**, 461–480.

Randall, D. A., 1980: Conditional instability of the first kind upside down. *J. Atmos. Sci.*, **37**, 125–130.

Rodts, S. M. A., 2001: *Shallow cumulus dynamics: Observations and parameterization*. Master's thesis, Utrecht University, Utrecht, 78 pp (Available from Utrecht University, Utrecht, The Netherlands).

Rodts, S. M. A., P. G. Duynkerke, and H. J. J. Jonker, 2003: Size distributions and dynamical properties of shallow cumulus clouds from aircraft observations and satellite data. *J. Atmos. Sci.*, **60**, 1895–1912.

Rogers, R. R. and M. K. Yau, 1989: *A short coursee in cloud physics*. Butterworth-Heinemann, third edition edition, 290 pp.

Siebesma, A. P., 1998: Shallow cumulus convection. *Buoyant Convection in Geophysical Flows*, E. J. Plate, E. E. Fedorovich, D. X. Viegas, and J. C. Wyngaard, eds., Kluwer Academic Publishers, volume 513, 441–486.

Stull, R. B., 1988: *An Introduction to Boundary Layer Meteorology*. Kluwer Academic Publishers, 666 pp.

Wang, Y. and D. A. Randall, 1996: A cumulus parameterization based on the generalized convective available potential energy. *J. Atmos. Sci.*, **53**, 716–727.

Warner, J., 1955: The water content of cumuliform clouds. **7**, 449–457.